DELINEATION OF SOLID MINERAL STRUCTURES WITHIN PART OF NASARAWA STATE NIGERIA FROM AEROMAGNETIC AND AERORADIOMETRIC DATA

BY

IBEZIM, Uchenna Chidiebere
MTech/SPS/2017/7026

DEPARTMENT OF PHYSICS
FEDERAL UNIVERSITY OF TECHNOLOGY,
MINNA

SEPTEMBER, 2021

DELINEATION OF SOLID MINERAL STRUCTURES WITHIN PART OF NASARAWA STATE NIGERIA FROM AEROMAGNETIC AND AERORADIOMETRIC DATA

BY

IBEZIM, Uchenna Chidiebere
MTech/SPS/2017/7026

A THESIS SUBMITTED TO THE POSTGRADUATE SCHOOL FEDERAL UNIVERSITY OF TECHNOLOGY, MINNA, NIGERIA IN PARTIAL FULFILMENT OF THE REQUIREMENTS FOR THE AWARD OF THE DEGREE OF MASTER OF TECHNOLOGY (M.Tech) IN APPLIED GEOPHYSICS

SEPTEMBER, 2021

ABSTRACT

Aeromagnetic data was analysed and used to delineate the structural features of the upper part of Nasarawa State of Nigeria which consists of Kuje, Keffi and Akwanga. These structural features include: lineaments, faults and folds which are channels for the accumulation of solid minerals. In delineating these structural features, some enhancement techniques such as horizontal derivatives, first vertical derivative and analytical signal were employed. Concentration maps were produced for the three radioelements viz Potassium (K), Thorium(Th) and Uranium (U). Furthermore , a ternary map and K/Th, U/K and U/Th ratio maps were produced. The residual magnetic intensity (RMI) map showed regions of different magnetic susceptibility which correspond to different lithology and depth of source rock. The RMI values range from -25.0 to 110.7 nT. The high magnetic signature occupied mostly the north-eastern and south- western part of the map corresponding to Akwanga and Kuje area respectively. The extreme south-eastern part of the map which is the sedimentary region has low magnetic intensity. The horizontal derivatives showed that most part of the area is characterized by a mixture of low and high magnetic closure of short wavelength that are high in frequency of occurrence. Few areas with relative sedimentation are denoted with averagely long wavelength. The analysis of the first vertical derivative map revealed fault zones, lineaments and intrusions. These lineaments trend in the NE-SW direction while the fault lines trend mostly in the NE – SW and E – W directions. The analytical signal showed amplitude range of -119.1255 - 28.4702 nT/m. Most of the lineaments, faults and intrusions observed in the map have high analytical signal. Low analytical signal was observed on the sedimentary region .The K/Th ratio map showed high K/Th ratio in the biotite-granite region having contact with the sedimentary rock in the south-eastern part of the map. Also the long stretch of lineament located towards the south-western area at Longitude 7.24^{o}E-7.25^{o}E and Latitude 8.30^{0}N-8.50^{0}N has high K/Th ratio while the sedimentary region at the extreme south-eastern part of the map has low K /Th. These areas of high K/Th ratio indicate regions of hydrothermal alteration which are possible areas of gold mineralization. The ternary map confirms the region of hydrothermal alteration indicated in the K/Th ratio map .The ternary map also showed that the biotite granite intrusions at Longitude 7.46^{0}E-8.03^{0}E and Latitude 8.30^{0}N-8.34^{0}N and the one located at Latitude 8.44^{0}N-8.50^{0}N and Longitude 8.20^{0}E-8.30^{0}E have high concentration of K,Th and U. The magnetic lineaments that represents fractures where hydrothermal alteration took place are potential hosts of gold minerals. Rocks in areas of high magnetic anomaly associated with these fractures are conduits for solid mineral accumulation.

TABLE OF CONTENTS

LIST OF TABLE

LIST OF FIGURES

CHAPTER ONE

1.0 INTRODUCTION

1.1 Background to the study

Potential field methods of geophysical survey such as the magnetic and the radiometric methods have been useful in investigating subsurface geological structures. They have also been useful in giving information about the basement rocks and geologic structures like fractures, faults and contacts which may have influenced the occurrence of mineralized rocks. Magnetic survey has been extensively used to delineate subsurface structures and provide an estimate of the thickness of non- magnetic sediments overlying magnetic rocks. However, the interpretation of magnetic data can be ambiguous due to the dipolar nature of the magnetic field and the direction of magnetization in rocks. Despite these complications, magnetic surveys and their interpretations can give very useful geological information when applied to the right types of problems (Ahmed *et al.*, 2012). Magnetic variation or susceptibility may be analysed using either total intensity or residual maps. Detailed geologic features such as the geometry and configuration of individual basement blocks can be shown by magnetic residual maps. They bring out the subtle magnetic anomalies that result from the changes in rock type across the basement rocks. On the other hand, total magnetic intensity maps show large scale geologic features such as basin shape or anomalous rock types within the basement (Nettleton, 1962). Generally aeromagnetic maps reflect the variations in the magnetic field of the earth. These variations are related to structural and magnetic susceptibility change (Ozebo *et al*., 2014).

Aeromagnetic survey is one of the geophysical survey techniques carried out using a magnetometer attached to an aircraft and flown within the survey area. This enables quick coverage of much larger areas of the earth's surface . The resulting magnetic maps shows the spatial distribution and relative abundance of magnetic minerals (Most commonly magnetite) in the upper levels of the crust. The magnetic map shows the geology and the geological structures of the upper crust of the earth. This is very helpful where bedrock is hidden by thick sediments. The aeromagnetic method is very useful in mineral exploration as it helps to delineate structures like faults, folds, contacts, shear zones and intrusions which are favourable areas for mineral deposits. These structures play important roles in the localization of minerals. Areas that are affected by deep weathering and thick overburden usually complicate the problem of rock delineation. One of the ways to achieve greater accuracy in facies delineation is by the use of radiometric method (Amadi *et al*., 2012)

The radiometric method measures the naturally occurring radioactive materials that emits the ionization radiation (the alpha (α), Beta (β) and gamma (γ)) from rocks. Out of these ionization radiations mentioned, the gamma rays have the highest penetration power and are used in radiometric survey. In the field, the gamma rays are detected by a spectrometer coupled with the scintillation detector. Theoretically, the energy of the gamma rays emitted from the natural radionuclides range from 0 to 3 MeV, but in the geological survey, the interest lies between 0.2 and 3 MeV (Kearey *et al*., 2002). Peaks in the spectrum are attributed to potassium (%K), thorium (eTh) and uranium (eU). The count rate of the whole spectrum is referred to as the total count (TC). The rocks near the earth surface are often weathered. During weathering thorium is often freed by the breakdown of minerals and may be remained in Iron (Fe) or Titanium (Ti) oxides/hydroxides and with clays. Uranium is a reactive metal and easily removed from

the origin places. It may be present in rocks as oxide and silicate minerals, uraninite and uranothorite; as trace amounts in other minerals or along grain boundaries possibly as uranium oxides or silicates (Kearey *et al*., 2002; Milsom, 2003).

The radiometric method is one of the most cost-effective and rapid techniques for geochemical mapping based on the distribution of the radioactive elements: potassium, uranium and thorium. The method is very useful for geological mapping and exploration of other types of economic minerals. It is also applied in geochemical and environmental monitoring such as the detection of radioactive contamination as a result of nuclear accidents and environmental pollution. It allows the interpretation of regional features over large areas, and applicable in several fields of science (IAEA, 1991; 2003). They may be used to estimate and assess the terrestrial radiation dose to the human population and to identify areas of potential natural radiation hazard. Regional surveys also provide a baseline data set against which man-made contamination can be estimated. The airborne radiometric datasets can also provide detailed information about the characteristics of the soil and its parent rocks, including surface texture, weathering, leaching, soil depth, moisture, and clay mineralogy (Bierwirth, 1997).The airborne radiometric data may be less reliable in urban areas because a significant proportion of the ground area is covered with buildings and/or asphalt paving, and the flight altitude is approximately 240 m. As a result of that, the number of gamma ray from the Earth that reach to the detector resulting from the measured concentrations of eU, eTh and K for the urban area are very low (Appleton *et al*., 2008).

In this study, aeromagnetic and radiometric datasets of the study area were acquired, processed and interpreted and areas with high potentials of minerals were delineated.

The Total Magnetic Intensity (TMI) map of the study area was produced and interpreted to indicate regions of high and low magnetic susceptibility. The aeromagnetic were passed through various filtering methods and the results were used to delineate geology structures like faults, folds and veins which are possible hosts of solid minerals.

On the other hand, the radiometric data were used to produce the Potassium (K), Uranium (U) and Thorium (Th) concentration map to delineate the regions of highs and low concentration of these elements. Also radiometric ratio maps (K/U, Th/U, Th/K and U/K) were produced and these were compared and related to indicate areas where there are veins. Finally a Ternary map was produced by merging the data of potassium (red), Thorium (green) and Uranium (blue) and correlating it with geology map of the area. The Ternary map gives the picture of the concentration of the elements combined together.

1.2 Statement of the Research Problem

The dwindling and fluctuating price of crude oil is biting hard on the Nigeria economy. Therefore, there is a great need to diversify and explore the solid mineral sector which can help boost the Gross Domestic Product (GDP) of the country.

The problem this work tries to solve is to use the aeromagnetic and aeroradiometric data to interprete possible geology structures (fractures, faults, folds and shear zones) that could be possible host of gold deposits and evaluate the exact position where these minerals are available.

1.3 Aim and Objectives of the Study

The aim of this study is to identify potential regional structures with possible solid minerals (gold) deposits in part of Nasarawa state through the use of aeromagnetic and aero-radiometric data interpretations.

Objectives

The objectives of the study are to:

1. Compare the residual magnetic intensity map with the geologic map to reveal major geological features, magnetic trend and susceptibility variance.
2. Delineate geological structures and lineaments within the study area by computing the analytical signal, horizontal and vertical derivative within the field.
3. Delineate regions of hydrothermal alteration from ternary map and ratio maps and to correlate the structures obtained from first vertical derivative map with that obtained from the ternary map and geology maps.

1.4 Justification of the Study

There is an agitation for economic restructuring of Nigeria which suggests that every state should manage a large chunk of their resources. Nigeria is blessed with abundant mineral resources that if well harnessed, every part of the country will develop its resources and be self-sustaining, thereby reducing these agitations to the barest minimum hence the need for this study.

CHAPTER TWO

2.0 LITERATURE REVIEW

2.1 Review of Geology of the Study Area

The study area is covered with 95% Basement complex rocks while the remaining 5% is made up of sedimentary rocks. The Migmatite-Gneiss intricately associated with the older Granite occupy the areas of Karu, Gurku, Panda, Gitata to the Northwest, Keffi, Garaku Akwanga and Nasarawa Eggon to the north-central and Wamba, and environs to the northeast (Obaje, 2009). Sedimentary rocks of Cretaceous-Tertiary ages cover greater part of Nasarawa State in the South beginning from areas around Lafia, Doma through Obi, Jangwa, Awe and Keana. Eggon and Kokona; Salt deposits in Ribi, Keana and Awe; Limestone deposits at Adudu, and Jangwa; at Keffi, Akwanga, NasarawaEggon, TuduUku, etc. (Obaje, 2007).

Ekeleme *et al* (2017) in their geologic investigation of rocks at Angwan Madaki in Nasarawa state, North central Nigeria identified the rock types in the area to include the Precambrian gneisses, granite and porphyroblastic gneiss, banded gneiss and migmatites with characteristic pegmatites and vein intrusions. These rocks experienced various tectonic episodes which resulted to their different structural styles such as mineral lineation, foliation, jointing, veins, faults, dykes and minor folds (Ekeleme *et*

al., 2017) .The geological mapping of the area revealed five dominant lithologic units namely; migmatites, banded gneiss, granite and porphyroblastic gneiss,older granites and dolerite respectively. Structural mapping carried out by the same researchers confirmed the presence of different folds such as crenulation and ptygmatitic fold. Other structures such as dykes, joints, quartz veins, fractures and micro-faults were detected on the rocks. They affirmed that the overall result showed that the study area is a manifestation of pan African deformation are revealed by the magnitude and style of the folding and other structural features of rocks in the area.

Many workers on a regional scale have carried out researches on the Basement Complex. Among these researchers is Falconer (1911), who first studied the Nigerian Basement Complex and distinguished the Younger Granite from the Older Granites. In one of the early records of the mineral survey, the occurrence of pegmatite, cassiterite and columbite-tantalite was mentioned though not much attention was given to the pegmatite from which they were derived (Jacobson and Webb, 1946). Oyawoye (1964) classified the Basement rocks as Older Meta-sediments, which includes Gneiss, Migmatites and Older Granites and Younger Meta-sediments. In reviewing the Basement geology of the Precambrian to Lower Paleozoic rock of Northern Nigeria, four major groups were recognized by Mc Curry (1976) viz ;

i. An underlying high amphibolite facies complex of quartzo-felspathic biotite and hornblende gneiss, migmatites and high grade meta-sedimentary relics comprising of older, meta-sediments.
ii. A supracrustal cover of low to medium grade meta-sediments.
iii. A suit of post syntectonic to late syntectonic granitoids, the older Granite intrudes the crystalline complex and the belts unto the younger meta-sediments.

iv. Volcanic rocks belonging to the Post Pan-African (Older Granite) episode of high level magmatic activity.

Oyawoye (1964), succeeded in subdividing the Basement Complex rocks into three major groups which he described as (a) the older meta-sediments, consisting of calc-silicate rocks. He considered this group as the oldest rocks of the Basement Complex. (b) The Gneisses, Migmatites and the older granites. In this group, two major types of gneisses were identified: the biotite gneiss and the banded gneiss. He also grouped the migmatites into two types, namely; the lit-par-lit gneiss and the migmatitic gneiss. On the basis of petrography, he suggested that the gneisses and migmatites originated through silica-potash metasomatism.

The Geological Map of Nigeria by Okezie (1974) shows that the Precambrian Basement Complex can be divided into two distinct zones, namely: a western zone in which the N-S trending elongate Schist belts are seperated from one another by Migmatite Gneisses and Granites, and an eastern zone, comprising mainly Migmatite Gneisses and granites, in which the Schist belts are scarcely present.

Cooray (1974) in further review added another family of rocks (the intrusive) to the works of Oyawoye (1964). He further effected some changes in the conclusions of Oyawoye (1964) such as (a) that the Older granites and related charnockitic rocks are of intrusive rather than metasomatic origin; (b) the Older granites and granodiorites based on the relative time of emplacements and deformation are subdivided into; syn-tectonic microcline-megacrystic, partly foliated granites and late- tectonic, less richly megacrystic, weakly foliated xenolithic granites and granodiorites with cross-cutting contacts and occasional thermal aureoles (McCurry and Wright, 1971; Jones and Hockey, 1964); (c) the north-south to northeast-southwest structural pattern in the Basement Complex has been pointed to have resulted from polyphase metamorphism

which has affected the Basement Complex leaving an imprints of at least three plutonic events during the Eburnean, Kibaran and the Pan-African orogenic episodes (Grant, 1978). Rahaman (1988) had described the rocks of the Schist belt as composed of predominantly metamorphosed pelitic to semi-pelitic rocks, granites, sandstones, polymeta- conglomerates, calcareous rocks, mafic to ultramafic rocks with minor amounts of greywacke and acid to intermediate volcanic rocks.

Umeji and Caen-Vachette (1991) reported that the Basement Complex in the vicinity of Nassarawa-Eggon which is several kilometers North East of the study area contains granitic gneisses, gneissic granites and occasional lenses of amphibolites. They reported that the Pan-African tectonics imposed NE-SW to ENE-WSW trends on all the rocks and that the Basement Complex is locally sheared with a mylonitic shear zone (340 m).

The schist belts occupy N-S trending synformal troughs and such troughs have been identified and described (Ekwueme, 2003). According to Obiora (2005), the schistose components of the migmatitic terrain were designated, “the older meta-sediments” while the distinct N-S trending schist belts, which are clearly younger than the gneisses and migmatites were mapped as “the younger meta-sediments”. Important to note is that the Older Granites occur intricately in association with the Migmatite-Gneiss Complex and the Schist Belts into which they generally intruded. This means that the rocks occur in most places where rocks of the Migmatite-Gneiss Complex or of the Schist Belt occur (Obaje, 2009) (Figure 2.1). In Nigeria, the Precambrian Basement Complex is exposed in five major locations, namely: North- eastern zone, South -western zone, South-eastern zone (extension of the Bamenda Massif into Nigeria), North-eastern zone called the Hawal massif and South-south-eastern zone also called the Oban Massif (Obiora, 2005). The Geology map of the study area is shown in Figure 2.2.

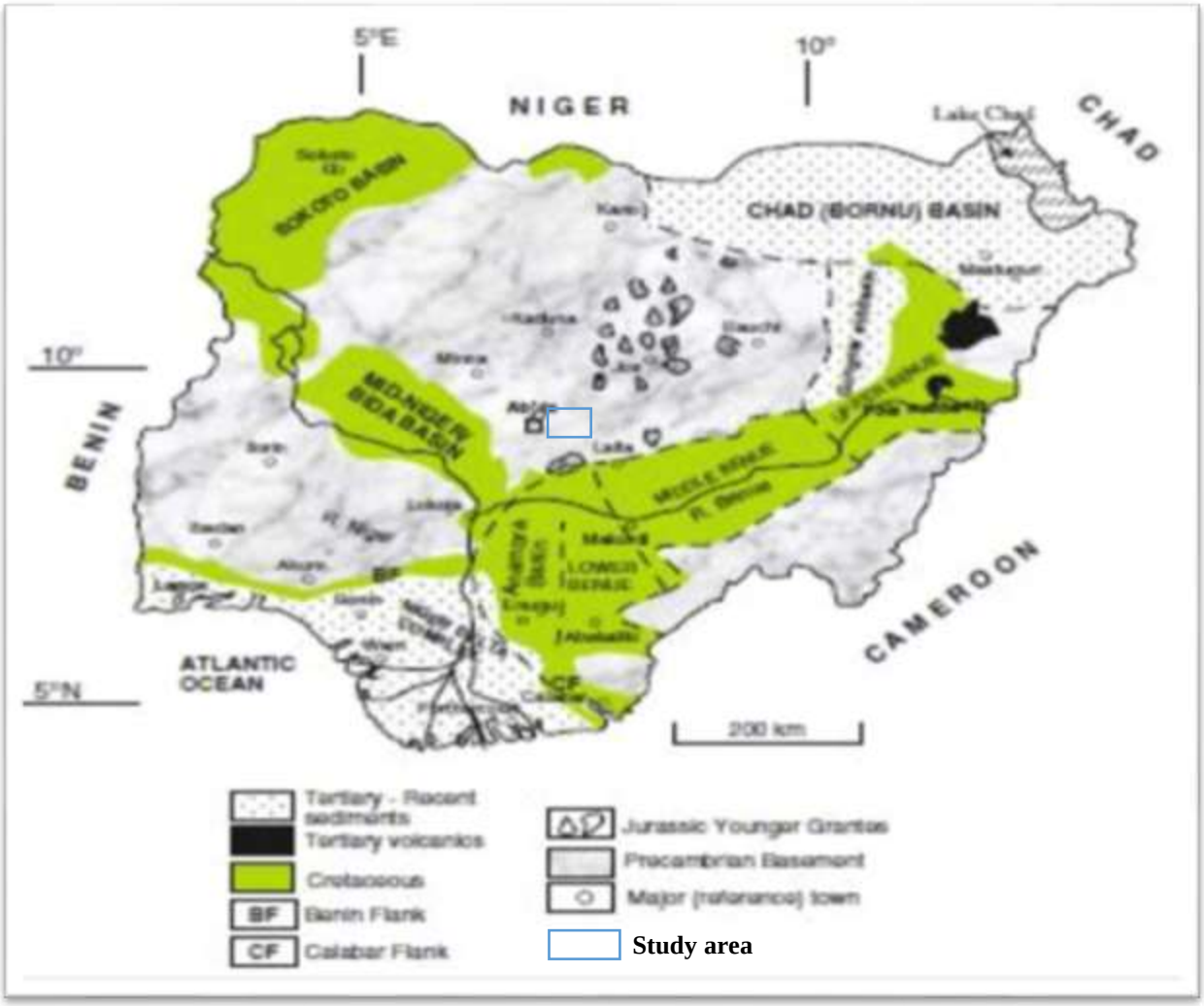

Figure 2.1: Geology map of Nigeria showing the location of Study Area (Adapted from Obaje, 2009)

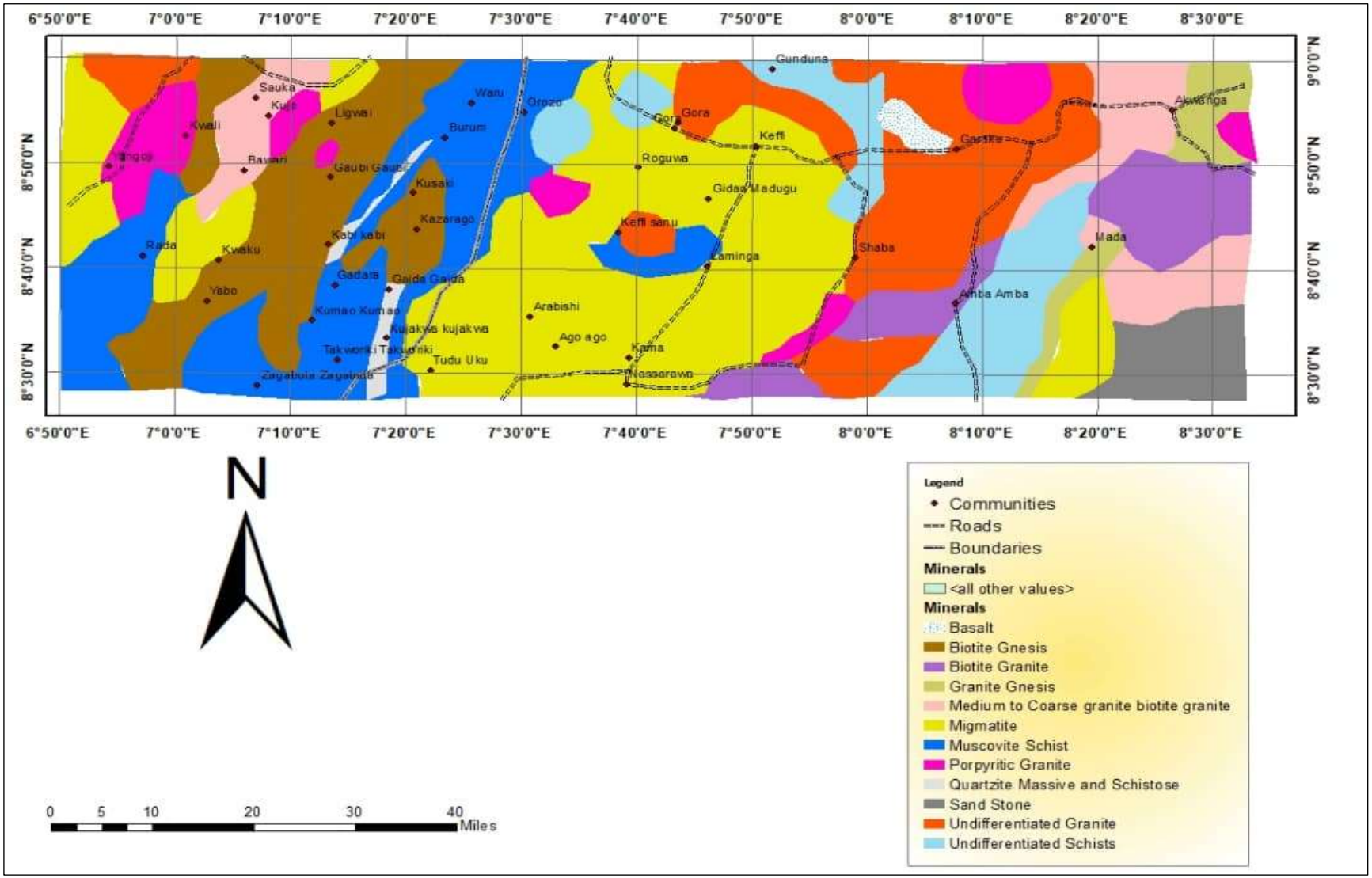

Figure 2.2: Geology Map of the Study Area

2.2 Earth's Magnetism

The earth is divided into three parts namely: Crust, Mantle and Core (Figure 2.3). The Core is the innermost part of the earth and it is divided into two parts viz: the molten outer core and the solid inner core. Reeve (2010) indicated that the movement of the charged electric particles within the molten core produces a magnetic field around the Earth. This magnetic field enveloping the Earth gives rise to the magnetic features of the various rocks found within or on the surface of the Earth.

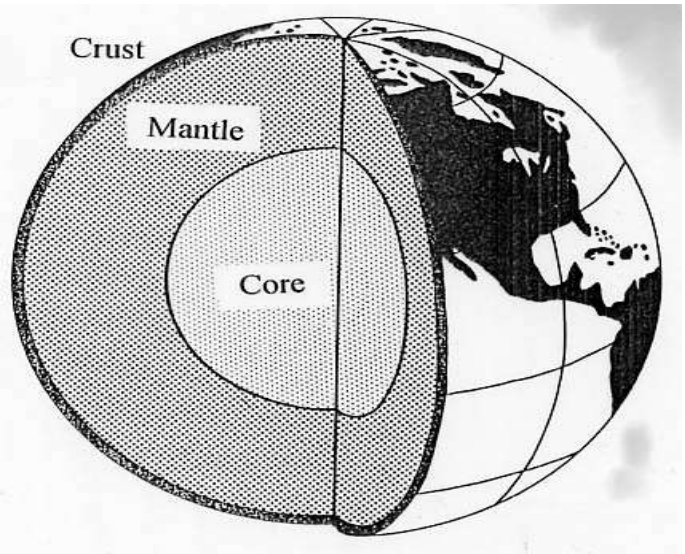

Figure 2.3: Internal Structure of the Earth (adapted from Reeves, 2005).

Close to the magnetic equator of Earth, the ambient magnetic field is almost horizontally oriented approximately north-south, and has a field intensity of between 25000 and 40000 nT, about one-half the intensity at the magnetic poles. The magnetic equator lies within 10^{o} of the Earth's geographic equator. The decreased equatorial field intensity causes local magnetic anomalies at low latitudes to have smaller magnitudes than those produced by similar structures at high latitudes. The north-south orientation of the horizontal inducing field means that a long north-south striking magnetic structure may show no anomaly at all, except at the south and north termination of the structure (Beard and Goitom, 2000). On the other hand, the outcome can be generally

reviewed this way; magnetic readings are high along and near a line that goes through a magnetic object in the direction of the field of the Earth; magnetic readings are low in all other locations. Additionally, at very low latitudes, typically between 10^{o} inclinations, the amplitude correction for north-south trending features unduly intensifies noise and alters difference in the magnetic susceptibilities from originating magnetic sources in different directions from the external field. There are always complications with magnetic dataset interpretations because of the asymmetric anomalies produced by symmetric causative rocks mostly located anywhere on the Earth apart from areas closer to the magnetic poles (Rajagopalan, 2003).

In exploration Geophysics, the geomagnetic field (Figure 2.4) of the Earth is composed of three parts (Telford, 1990).

a. The main field which varies relatively slowly and is of internal origin.
b. A small field (compared to the main field), which varies rapidly and has its origin outside the Earth. This is also called external field.
c. Spatial variations of the main field, which are usually smaller than the main field. They are constant in time and place and are caused by local magnetic anomalies in the near-surface crust of the Earth. These are the targets in magnetic prospecting. The compass needle aligns itself in the direction of magnetic field of the Earth when hanged freely at any position on the surface of the Earth. This alignment creates an angle between the magnetic and geographic north (Kearey *et al.,* 2002). The Geomagnetic elements are: Inclination and declination. Declination can be defined as the angle the geographic north makes with the magnetic north of the Earth while magnetic Inclination is the angle the total field Vector makes above or below the horizontal plane (Reeves, 2005).

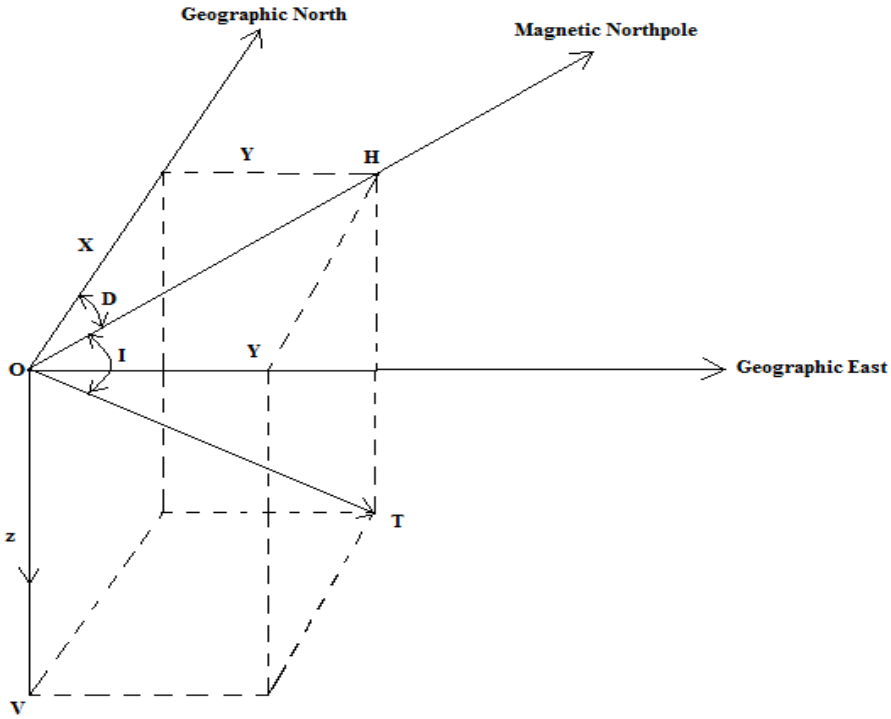

Figure 2.4: Vector representation of the geomagnetic field at any place on the Northern Hemisphere (Whitham, 1960).

From figure 2.4 above, the magnetic field is a vertical plane, It is passing through the total magnetic force "T". Therefore, the magnetic field of the Earth at every position on the surface of the Earth "V" and "H" are vertical and horizontal components of the magnetic field .These magnetic elements (according to Roy, 2008) can be related as follows:

$$H = TcosI \qquad 2.1$$

$$V = TsinI \qquad 2.2$$

Where, I is the angle of inclination.

2.2.1 Magnetic susceptibility

The degree to which a material can be magnetized in an applied external field is a physical parameter known as magnetic susceptibility (Dalan, 2006). In geology, magnetic susceptibility is one characteristic of a mineral type. Its measurement gives us information about the type and quantity of minerals present in the sample. The measure

of magnetization is solely characterized by the amount and composition (shape and size) of iron oxide in the rocks (Dearing, 1994; Wemegah *et al*., 2009).

The magnetic susceptibility effectively is the magnetization effect divided by the applied magnetic field. If the magnetic field is **H** (A/m) and the magnetization is **M** (A/m), the magnetic susceptibility is:

$$\kappa = Xv = M/H \qquad 2.3$$

Where X_v is volume of susceptibility

According to Reynolds (1997), most sedimentary rocks contain negligible quantities of magnetic minerals, and are therefore non-magnetic. Most basic igneous rocks, on the other hand, have high magnetic susceptibilities, while acid igneous rocks and metamorphic rocks can have susceptibilities ranging from negligible to extremely high. Magnetic susceptibility is a trace parameter of rocks, because the percentage of magnetic minerals is usually one percent or less, even in basic igneous rocks. Slight differences in iron oxide content of a mineral can cause large magnetic susceptibility variations. Reeves (1989) also pointed out that the amount of iron oxides in rocks are influenced by the parent rock, age of rock and weathering processes.

2.2.2 Remanent and induced magnetism

There are two components involved in a rock's magnetization that is remanent magnetism and induced magnetism. Remanent magnetism also known as the permanent magnetism is the type which when the applied field is removed, still remains in the rock. Ferromagnetic materials retain their magnetism even when the external field is taken away. Rock magnetization usually takes place mostly at the shallow depths because there is an increment in temperature towards the centre of the Earth (typically < 50 km depth) (Clark and Emerson, 1991). Furthermore, remnant magnetization can occur when the arrangement of the magnetic domains are locked in the presence of a

weak geomagnetic field. During cooling, the magnetic domains are locked up at specific curie points owing to significant change in crystal growth.

Magnetizations are little and influence only the most sensitive magnetic sensors (Reeves, 1989). Primary remanent magnetization is acquired by the cooling and solidification of an igneous rock from above the Curie point (of the sources of magnetic minerals) to normal surface temperature or by detrital remnant magnetization (DRM). Secondary remnant magnetization, such as chemical, viscous or post-depositional remnant magnetization, may be acquired later on in the rock's history (Reynolds, 1997). The magnetization effect, M divided by the applied effect; H gives the magnetic susceptibility of the rocks. This explains best Induced magnetization (Reeves, 1989).

2.2.3 International geomagnetic reference field (IGRF)

The international Geomagnetic Reference field defines the theoretical undisturbed Magnetic field at any point on the Earth's surface in simulating the observed Geomagnetic Field by a series of dipoles. This formula is used to remove from the magnetic data those magnetic variations attributable to this theoretical field. The IGRF provides the means of subtracting on a rational basis the expected variation in the main field to leave anomalies that may be compared from one survey to another, even when surveys are conducted several decades apart and when, as a consequence, the main field may have been subject to considerable secular variation (Reeves, 2005). The IGRF is published by a working group of the International Association of Geomagnetism and Aeronomy (IAGA) on a five-yearly basis. A mathematical model is advanced which best fits all actual observational data from geomagnetic observatories, satellites and other approved sources for a given epoch. Software is available which permits the use of these coefficients to calculate IGRF values over any chosen survey area. The values currently in use are based on the IGRF 2015 and its tentative extrapolation (prediction)

to 2020. Once all relevant actual observations (as opposed to predictions) have become available, it is possible to revise the prediction and announce a definitive reference field. It is normal practice in the reduction of aeromagnetic surveys to remove the appropriate IGRF once all other corrections to the data have been made. Departures of the subtracted IGRF from an eventual definitive IGRF may need to be considered when re-examining older surveys retrospectively. From the point of view of exploration geophysics, undoubtedly the greatest advantage of the IGRF is the uniformity it offers in magnetic survey practice since the IGRF is freely available and universally accepted.

2.2.4 Units of magnetism

The unit used in geomagnetic survey is in Tesla

a. 1Tesla = 1T = 1N/Am
b. 1nT =10^{-9}T = 1γ =10^{-5} Oersted
c. C.g.s (Centimetre-gramme-second) unit

   1 gauss (G) =10^{-4}T

   1 gamma (γ) =10^{-5} G

2.3 Review of Previous Works

Joseph *et al* .(2019) , Interpreted high resolution aeromagnetic and satellite data covering part of Maru Schist belt in Zamfara state, north-western Nigeria in order to understand the distribution of the surface and sub-surface magnetic materials within the study area, delineate geologic lineaments and estimate the depth of magnetic sources. Results of the satellite map the analytical signal and horizontal derivative filters applied to the residual magnetic intensity data revealed that the Maru Schist belt contains highly magnetic minerals suspected to be Iron. Further result of the analysis showed that the structural lineaments predominantly trending NW-SE within the area are also evident. The researchers inferred that the Maru schist belt has shown the presence of

hydrothermally altered iron mineralization (Ferric and Ferrous) distributed at various degree round the study area.

In the same vein, Daniel *et al.* (2019) conducted a research aimed at delineating and characterizing subsurface geologic structures in Shanono, Kano state Nigeria using high resolution aeromagnetic data. The researchers applied Euler's solution of the aeromagnetic data with structural index one and the result revealed the presence of the major tectonic trends of anomalies in the NE-SW and the NW-SE directions. They observed that the trends of some of these structures are similar to fracture orientations in the Nigerian Basement Complex rocks. They were of the opinion that these structures control the emplacement of the gold mineralization as these provides the pathways of flow of mineral-rich fluid within the host rocks of the study area.

Olomo *et al* (2018) investigated the mineralization potential of Iperindo and its environs using satellite remote sensing and geophysical methods. Their area of study lies within Ilesha Schist belt of the Precambrian basement complex of South-western Nigeria. Their investigation involved the use of extracted lineament from Landsat Thematic Mapper Imagery to compliment results of interpreted magnetic field intensity over the study area. The researchers interpreted the aeromagnetic data of the area using spectral analysis and Euler deconvolution of the processed magnetic anomaly map over the area. The enhancement techniques they used include: reduction to equator wavelength, upward continuation and derivative filters. The processed Images revealed lineaments trending majorly in NE-SW directions, diagnostic of primary structures of potential targets for mineralization in the area. The researchers also observed a coincidence of both Landsat and aeromagnetic lineament trends in the study area which according to them, suggested that these lineaments reflect real continuous fault/fractures in depths

Ademila *et al.* (2018), carried out a research using radiometric method to investigate the radioactive properties of rocks in parts of South-western Nigeria with a view to interpreting the geological structure and abundance of natural radioactive elements in rocks. The airborne radiometric dataset of Ikole sheet and the ground radiometric data were recorded from eight traverses in the Akoko axis of the study area. The results were presented as maps and it showed moderate to very high concentrations and very low to low concentrations of the radioelements : Uranium (4.5-13.0ppm); (LLD- low limit of detection-3.0ppm), Th (25.0-70.0ppm);(8.5-16.0ppm) and K(2.0-4.0%); with the most often observed values in the range 2.5-7.0ppm, 22.0-30.0 ppm and 3.0-4.0% for U, Th and K respectively.

Rowland and Nur (2018), in their interpretation of high resolution aeromagnetic data over Nasarawa area synthesized interpretative maps derived from first vertical derivative and analytical signal along with depth estimates. They identified series of fault fracture trends such as NE-SW, NW-SE, NNE-SSW, NNW-NNE, E-W and N-S directions. The NE-SW is the dominant trend in the area. Faults were interpreted along linear aeromagnetic anomalies and breaks in anomaly patterns. The interpreted faults showed criss-crossing pattern of fault zones, some of which appear to step over where they cross, and show zones of west-northwest, around akiri warm spring. North easterly striking faults extend east from this juncture. The researchers opined that the associated aeromagnetic anomalies are likely caused by magnetic contrasts associated with rifting of crust beneath the Benue Trough. Also result from the Analytical signal revealed the predominant NE-SW trend. A low magnetic susceptibility of 0.01nT was observed at the south-eastern part of the study area which they said corresponds with thick sedimentary sequence, while magnetic anomalies of 0.2047nT correspond with the volcanic intrusion at the extreme north and south-eastern part of the study area.

Sayeed and Mahmoud (2018) carried out a study in part of central-eastern desert, Egypt using airborne magnetic and radiometric data. Their study was aimed at locating probable gold mineralization zones in a selected part of the central–eastern desert of Egypt. To achieve this result, they used both aeromagnetic and aero-radiometric data in their analysis. Some enhancement techniques were employed by these researchers which include First Vertical Derivative, Analytical Signal and both Centre for Exploration Targeting (CET) grid and porphyry. Radiometric maps were also used to aid the the interpretation process. The results indicated that the study area is dominant by NW, NNW, NNE, WNW, NE, E-W and N-S structural directions. They considered the NW-SE as the most important trend and also regarded as the preferred orientation of ore deposits. They mapped a number of hydrothermal alteration zones within younger granite; Hammamat felsites and metasediments.

Ejepu *et al* (2018), employed integrated geosciences techniques to prospect for gold mineralization in Kwakuti, North-Central Nigeria. The employed geosciences techniques include: surface geological mapping, processing and analysis of aeromagnetic total magnetic field intensity data using Oasis Montage software and x-ray fluorescence analysis of soil samples. Migmatites and Gneiss were seen to dominate the rock outcrops in the area. The Migmatites displayed low magnetic field intensity values, while the Schist showed high magnetic field intensity values. The first derivative map of the magnetic field intensity data revealed NE-SW trending lineaments. Gold concentration distribution pattern in the study area is skewed NE-SW, thereby suggesting that the NE-SW structures control the mineralization.

Nwankwoala *et al.,* (2017) carried out a geological mapping of the Jos-Plateau area using aeromagnetic data and satellite image of the area based on structures. The aeromagnetic interpretation study revealed that the major strike direction in the study

area is NE-SW and characterized by magnetic anomalies ranging from 7630 to7950 nT. The predominant strike direction obtained from the satellite image of the study area trends NW-SE while the data measured in field (Rose plot) confirmed NE-SW, NW-SE trend. Their work revealed that the Basement Complex in north-central Nigeria is a polycyclic structure with probable different episodes of orogenic activities.

Similarly, Adewumi and Salako (2017) carried out a qualitative analysis of aeromagnetic data in some parts of Nasarawa state with the aim of delineating mineral potential zone. The vertical derivative, downward continuation and analytic signal data processing techniques were used. The First and second derivatives showed lineament trend of NE-SW. The downward continuation carried out continued at a depth of 50 m and100 m and the researchers were of the opinion that the veins are magnetic minerals. The research also revealed that the magnetic signatures ranges from -51.2 nT to 110.4 nT after the removal of IGRF value of 33000 nT. They observed that the high which is the basement dominates the north-eastern and north-western part of their study area which corresponds to Akwanga, Wamba and Nasarawa–Eggon. According to the researchers, these are areas with promising solid minerals of economic potentials, like gold at Wamba; Tin, Columbite and Tantalite at Akwanga while granitic rocks with possible radioactive elements are in abundance in Nasarawa-Eggon. The researcher's inferred that the low magnetic values on the other hand correspond with the region of sediment deposition dominate the southern part of the study area which includes Lafia, Keana and Doma.

Ohioma *et al.* (2017), analysed and interpreted the aero-radiometric data of Isanlu area of Kwara state Nigeria which is on sheet 225 (1:100000). The aim of their study was to delineate the hydrothermally altered zones that favour gold mineralization. The aero-radiometric data was subjected to filtering algorithm and enhancement techniques such

as shaded relief enhancement and elemental ratio enhancement using Geosoft Oasis Montaj software. They also used golden software surfer to identify and delineate the revealed hydrothermally altered zones. They were able to delineate eight hydrothermally altered zones from the enhanced aero data set. These hydrothermally altered regions include areas around Odogbe and Okolom in the north-central portion of the study area, and also Egbe in the western edge.

Obi *et al* (2015) studied the Bida basin, North central Nigeria using two aeromagnetic sheets with a scale of 1:100000 (sheet 184 and 185). They carried out both manual and computer processed analysis which involved map merging polynomial filtering lineament analysis and depth to magnetic source estimation. The result from manual lineament trend showed a major NW-SE dominant trend and a minor NE-SW trend.

Adetona and Abu (2015), conducted a study on the lower Benue and upper Anambra basins Nigeria, using Aeromagnetic data to determine the 2-dimensional models of the structural features within the study area. The analysis based on the Centre for Exploration Targeting (CET) showed that the basement rocks of the North and southern edge of the study area intrude into the sedimentary Formation. At the middle portion of the study area (within Angba and Otukpo sheets), structures that are basaltic intrude into the basement. The researchers also detected several fractures and fault lines on the CET map. The most prominent among them is that which starts from the eastern end (Latitude 7.45^{o} and longitude 8.30^{o}) and ends at the southern end (latitude 7.00^{o} and longitude 7.45^{o}), cutting the south-western corner of the study area diagonally. The 2-dimensional model of the six profiles revealed sedimentary Formations whose susceptibility values are zero (0). The basement susceptibility varies from 0.002 to 0.004 but in some places it was as high as 0.007 nT.

Moreso, Ogunmola *et al* . (2015), in their study of Wamba and Nasarawa-Eggon area of north-central Nigeria used high resolution aeromagnetic data alongside Nigeria Sat-X image to map out the major structural trends within the area. They performed the reduction-to-the- equator (RTE) operation on the aeromagnetic data after which horizontal derivative, analytical signal and tilt derivative were calculated to highlight subsurface boundaries and the major structures within the area. The researchers applied several digital image enhancement techniques such as general contrast stretching and edge enhancement to the Nigeria Sat-X image in ERDAS IMAGINE 9.2 after which structures from the interpreted magnetic data and the image were mapped out on screen using Arcmap 10. The results they obtained using the RTE produced a basement configuration that consists of several NE-SW and NW-SE structures that range from 1km to about 17 km in length with the NE-SW structures being the major trend in the area. They observed that the lineaments are mainly within the basement and the older granites and opined that it may be related to the Pan-African orogeny.

Adetona and Abu (2013), worked on the lower Benue basin and upper Anambra basin of Nigeria using both Spectral depth determination and source parameter imaging. In their study, some data processing operations were carried out on the aeromagnetic data which include: First vertical derivative, spectral depth analysis and source parameter imaging (SPI). They divided the survey area into forty–eight sections and ran Spectral depth analysis for each of the forty-eight sections and the result obtained showed that depth above 7 km was obtained within the cretaceous sediments of Idah, Ankpa and below Udegi at the middle of the study area. The researchers observed a minimum depth estimate of between 180.0 and 452 metres around the basement regions. The result they obtained from source parameter imaging revealed a minimum depth of 76.983 metres and a maximum thickness of sedimentation of 9.847 km which also occur within Idah,

Ankpa and Udegi axis. The observed structural trends within the study area using the first vertical derivatives are N-E and NE-SW. The magnetic Intensity of the area was gotten to be in the range of -2415.97 nT (minimum) to 1264.72 nT (maximum) with an average value of 33.87 nT.

Salako and Udensi (2013) also employed the spectral depth approach to analyse aeromagnetic data of parts of the Upper Benue Trough and Borno basin, North-Eastern Nigeria using aeromagnetic data. They analysed twenty-five aeromagnetic maps covering the study area which were digitized on a 3 km by 3 km grid and later compiled to produce a combined aeromagnetic data file for the area. The polynomial fitting method was applied by the researchers in the regional-residual separation. They subdivided the residual map into 41 spectral sections. The result they obtained showed that the first layer depth ranged from 2.06 to about 3.35 km.

Also, Adetona and Abu (2013) investigated the structures within the lower Benue and Upper Anambra basins, Nigeria using First Vertical Derivative, Analytical signal and Centre for Exploration Targeting (CET) plug-in. From the analysis of both the Vertical and Horizontal Derivatives, the study area could be divided into two regions based on the degree of distortion of the magnetic signatures. The northern and the western edge of the study area is covered by short wave length magnetic anomalous signatures that are the characteristics of outcrops and shallow intrusive magnetic bodies, while the remaining part of the study area is characterized by medium to long wavelength magnetic signatures of which the researchers said are attributes of deep-seated magnetic in areas of medium to thick sedimentation. Furthermore the result of the Analytical signal which is local amplitude according to the researchers revealed regions with outcrop of magnetic rocks having amplitudes ranging from 0.230 to 0.40. Also the researchers made the following observations: area with magnetic rock intruding into

sedimentary Formations at shallow depth, with amplitudes ranging from 0.094 to 0.229 cycles and regions with magnetic rock intruding into sedimentary Formations at greater depths, having very low amplitudes ranging from 0.085 to 0.055 cycles. The CET grid analysis equally revealed the basement rocks to the North and Southern edge of the study area. Intrusions into the sedimentary Formation were also revealed in the CET analysis. The researchers also discovered that the lower (Southern) part of the area (on Angba and Otukpo area) shows structures (Basaltic rocks) that intrude into the basement. Also several fractures and fault lines were detected on the CET map by the researchers, most prominent among them is that of the south-eastern corner of the area which trends NE-SW of which they attributed to be an onshore extension of Charcots fault zone, and that which trends N-S is a fault line that controls the course of River Niger.

Amadi *et al*. (2012) used the Gamma ray Spectrometer (DISA-300) and broadband Gamma ray Scintillometer (BGS-ISL) to evaluate the radiometric properties of rocks (Igneous, Sedimentary and metamorphic) in parts of South-Western Nigeria. They characterized the lithologies and observed that the concentration of radioactive elements in rocks varies. Shale, clay and granites were seen to have the highest number of gamma count (60-105) while amphibolites show the lowest count (16-46).

Aina and Olarewaju (2010) used airborne magnetic data and field observations to define structural trends in some parts of North-central Nigeria. They observed that the aeromagnetic anomalies of the Jurassic Younger Granite complexes are distinctive with relatively high amplitude and short wavelengths and inferred that they are directly associated with the outcrop patterns of the intrusions. They also observed that the Aeromagnetic data contain evidence of linear structural discontinuities and some of these linear features according to them are long and extend through the survey area.

They identified a pattern of contour offsets and also reflected deep crustal features cutting some of the Younger Granite known to be mineralized. A major fault was mapped which cuts the Ririwai complex of the East. They discovered that the fault trends NW-SE and appeared to extend southwards through the area. The regional trends of the structures were seen to be mainly Northeast- Southwest and Northwest-Southeast. The Northwest-Southeast trends according to the researchers were superimposed on the Northeast-Southwest trends. This they said suggests that the Northeast-Southwest lineaments are older than the Northwest-southeast lineaments patterns.

Collins, (2011) did a high resolution seismic reflection survey in Zaria, located in the Basement complex of northern Nigeria with the aim of mapping out the geologic structures that exist within the batholiths in order to determine their structural characteristics. The methodology employed by the researchers involved putting receivers at 1m interval and a constant offset distance of 1m was used for the survey. The researcher increased both the offset and the interval between the last receivers by 1m after taking each shot until the end of the profile was reached. He adopted a method which sampled a particular point for more than once within the subsurface, which resulted in a 12-fold data coverage for the 24 channel seismograph used. The result obtained showed that the discontinuous seismic events occurred mostly at the near surface, which showed that the upper part of the batholiths is highly weathered. The analysis of the extent of weathering showed that the batholith has weathered beyond a depth of 56 m, and that the average depth of the fresh basement is about 60 m. Most of the profiles showed area of fracturing within the overburden and the weathered Basement. The Basement topography was characterized by dipping structures which were arched upwards towards the granitic outcrops.

Talaat and Mohammed, (2010) carried out a survey in the Garin Hawal area of Kebbi state Northwest Nigeria using remote sensing techniques. They detected three main gold-bearing shear zones in the study area from the processed Landsat ETM+ images and extensive ground investigation. Extensive alteration zones were identified using high resolution Quick Bird image along Garin Hawal shear zone. They interpreted the alteration zones and associated quartz veins as generally concordant with the NE-SW regional structural pattern and dipping NW.

Akanbi and Udensi (2006), carried out a study in the Pategi area of Niger state to determine the structural trend and spectral depth analysis of the residual field using aeromagnetic data. The compiled magnetic map shows that an approximately NE-SW trending fabric characterizes the upper part of the area down to latitude 8.84^{o}N. This trend according to the researchers changes E-W in the central portion between latitudes 8.63^{o}N and 8.84^{o}N and below latitude 8.63^{o}N the trend changes again to approximately NE-SW particularly at the southwest fringe of the map. A major lineament depicting the Romanche paleo fracture zone was found in the area. Discontinuities and several magnetic closures of various sizes were observed in the map and these according to them indicate the presence of minor to moderately long fault zones in the area and the closures depict the sizes of the anomalies that lie beneath the basin.

CHAPTER THREE

3.0 MATERIALS AND METHODS

3.1 Location of the Study Area

The study areas are located in part of Nasarawa State, and Kuje in Federal Capital Territory, Abuja, North- Central Nigeria and are bounded by Longitude 7.0^{o}E – 8.30^{o}E and Latitude 8.30^{o}N-9.0^{o}N with an estimated dimension of 55x165 km (figure 1.1) . Nasarawa State is accessible by road through Kaduna and Plateau States to the North-East, Taraba state to the South-East, Benue State to the South, Kogi State to the west and Abuja to the North-West. The State is blessed with abundant mineral resources and for this reason it is tagged, ‘‘The Home of Solid Minerals in Nigeria”. The mineral deposits found in the state include: coal, barytes, salt, limestone, clays, glass sand, tantalite, columbite, cassiterite, iron ore, lead, gold and zinc (Idzi, *et al.,* 2013). The state has a population of 1,826,883 according to the 2005 population estimate. Nasarawa state is divided into thirteen Local Government Areas.

The general topography of Nasarawa State is that of hills/dissected terrain, undulating plains and lowlands. The southern local government areas of Nasarawa such as Awe, Doma, Nasarawa and Toto are bound by river Benue in the south. Its valleys and troughs extend inland for some 30 km and it is made up of flood plains laying generally below 250 metres. The flood plains further protrude inland along the coast of rivers Dep, Mada- Guma, Ayini and Farin-Ruwa which are the major rivers draining into the river Benue. The undulating plain has a general altitude of about 400 metres above sea level. Hills and dissected terrains occupy a sizeable portion of Nasarawa state. They are scattered all over the land mass with height range of between 600-1200 metres. The northern part of the state has a greater concentration with the Monkwa hills in the

northeast and the Mada rolling hills stretching from Wamba through Akwanga down to Nasarawa-egg on local government area.

Nasarawa state falls under tropical rainy climate. The rainy season span a period of seven months (April-October) with an annual rainfall of about 1200-2000 mm. The study area falls under the Guinea savannah vegetation zone which consists of tall grasses with scattered trees.

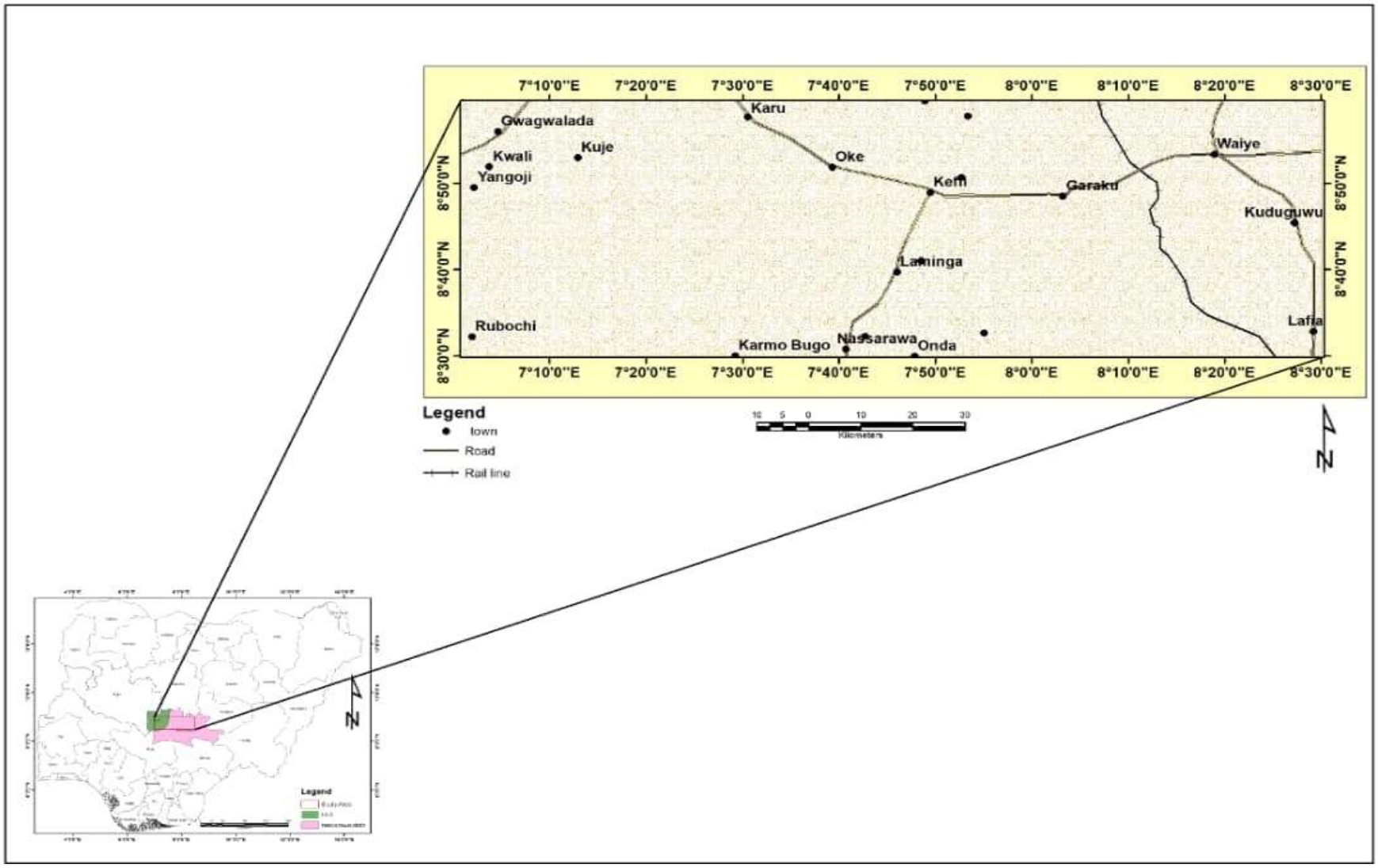

Figure 3.1: Location Map of the Study Area

3.2 Materials and Methods

The materials that were used for this work include:

a. Aeromagnetic data covering the study area
b. Radiometric data (Potassium, Thorium and Uranium)
c. Geology map
d. Geosoft (Oasis Montaj)
e. Microsoft Excel
f. Computer
g. Stationeries

The area of study lies between Latitude 8.30^0N – 9.00^0N and Longitude 7.00^0E – 8.30^0E with a total area of 9075 km^2. The total magnetic intensity data for this area is denoted by sheet 207 (Kuje), 208 (Keffi) and 209 (Akwanga). The radiometric data consist of eU, eTh and K equally represented by sheet numbers 207 (Kuje), 208 (Keffi), 209 (Akwanga).

Below are the procedures that were used in this Study:

1. Production of the residual magnetic intensity map of the study area to delineate the variation in magnetic susceptibility.
2. Application of reduction to equator and pole to remove the dependence of the data on angle of inclination and declination.
3. Obtaining the horizontal derivative maps of the study area to delineate contacts.
4. Computing the first vertical derivative in order to accentuate the structural features of the study area.
5. Evaluating the analytical signal so as to determine the exact position of the causative body.
6. Correlating the structures from FVD and Geology Map.

7. Analysis of Potassium K, Uranium U and Thorium Th concentration maps to delineate the regions of high and low concentration of the three radio-elements.
8. Production of radiometric ratio map K/U, Th/U, Th/K and U/K maps to delineate regions of hydrothermal alteration.
9. Production of ternary map to map geological boundaries and correlate with geology map.
10. Delineation of possible mineralisation zone within the study area through the structures obtained.

3.3 Source of Data

The data for this study were acquired from the Nigerian Geological Survey Agency (NGSA). The largest airborne geophysical survey was carried out in Nigeria in two phases between 2005 and 2009. The survey was partly financed by the Federal Government of Nigeria and the World Bank which was a part of a major project known as the Sustainable Management of Mineral Resources Project. Every aspect of this geophysical work which includes; data acquisition, processing and compilation was carried out by Fugro Airborne surveys. The survey acquired both magnetic and radiometric data. The survey has a tie line spacing of 5000 m, flight line spacing of 500 m and terrain clearance of 80 km using TEMPEST system. The flight line trend and tie line trend were 135 and 45 degrees respectively. The Sensor mean Terrain Clearance is 80 m and the Magnetic data recording interval is 0.1 second or less. The equipment used are aircraft Cessna Caravan 208B ZS-FSA, Cessna Caravan 208 ZS-MSJ and 3 x Scintrex CS3 Cesium vapour Magnetometer. This survey is intensive and more detailed for the objective of this research. The data covers the total number of sheets required for this work.

3.4 Theory of Method

Some of the theories backing up this research work are discussed below.

3.4.1 Filtering methods

Mathematical operations such as convolution and correlation can accomplish filtering residualizing, continuation and so on. Operations can be performed in the spatial or wave number domain (often called the frequency domain because wave number is spatial frequency) (Telford *et al.*, 1990). Some of the filtering operations that will be used in this research are explained below:

3.4.2 Fourier transform filter

Fourier transforms are very useful in magnetics (Telford *et al*., 1990) for

1. Changing the effective field inclination (pole reduction) or conversion of residual magnetic data to vertical-component data
2. Calculation of derivatives and general filtering/separation of anomalies caused by sources of different size and depth and modelling.

A much faster algorithm developed by Cooley and Turkey (1965) called the Fast Fourier Transform (FFT) is a competent mathematical tool used to calculate the Discrete Fourier transform (DFT) and its inverse. FFT algorithms can hence be regularly made into data processing programs so as to analyze spectral lines of the waveforms of geophysical data. Fourier transformations operate based on the operation of application program like Microsoft Excel for organizing, analyzing and storing data in the form of a table (Kearey *et al*., 2002).

3.4.3 Reduction to the pole (RTP)

Reduction to the pole transforms an anomaly into the anomaly that would have been observed if the magnetization and regional field were vertical (as if the anomaly was measured at the north magnetic pole). A symmetric body produces a symmetric anomaly at the magnetic poles. Hence, reduction to the pole is a way to remove the asymmetries caused by a non-vertical magnetization, or regional field, and to produce a simpler set of anomalies to interpret (Dobrin and Savit, 1988). The RTP technique is the best method and more commonly used for removing magnetic distortion. The resulting map shows a direct correlation between magnetic highs and their causative sources. It can only be applied to data that were acquired at magnetic latitudes greater than approximately 20° north or south.

3.4.4 Euler deconvolution

Euler deconvolution is a technique used for locating the source of a potential field, based on their amplitudes and gradients. The method was developed by Thompson (1982) to interpret 2D magnetic anomalies, and was extended by Reid *et al.* (1990) to be used on grid-based data. A magnetic field *M* and its spatial derivatives satisfy Euler's equation of homogeneity:

$$(x - xo)\,\partial M/\partial x + (y - yo)\,\partial M/\partial y + (z - zo)\,\partial M/\partial z = -NM \qquad 3.1$$

Where $\partial M/\partial x$, $\partial M/\partial y$ and $\partial M/\partial z$ represent first-order derivatives of the magnetic field along the *x*-, *y*- and *z*-directions, respectively; and *N* is known as a structural index and related to the geometry of the magnetic source. For example, $N = 3$ for a sphere, $N = 2$ for a pipe, $N = 1$ for a thin dyke, and $N = 0$ for magnetic contact (Reid *et al.*, 1990). Taking into account a base level for the regional magnetic field (*B*).

3.4.5 Vertical derivative

The vertical derivative is commonly applied to total magnetic field data to enhance the most shallow geological source and can be calculated either in space or frequency domain. The enhancement sharpens anomalies over bodies and tends to reduce anomaly complexity, allowing a clearer imaging of a causing structure. Then transformation can be noisy since it will amplify short wavelength noise. First vertical derivative data have become almost a basic necessity in magnetic interpretation projects. The second vertical derivatives has more resolving power than the first vertical derivatives (Milligan and Gunn, 1997).

$$L(r) = rn` \quad 3.2$$

Where n = order of differentiation.

3.4.6 Analytic signal

This is a filter applied to magnetic data and is aimed at simplifying the fact that magnetic bodies usually have a positive and negative peak associated with it, which in many cases make it difficult to determine the exact location of the causative body. Nabighian, (1972) has shown that for two-dimensional bodies, a bell shaped symmetrical function can be derived which maximise exactly over the top of the magnetic contact. The three dimensional case was derived in 1984 also by Nabighian, 1984. This function is the amplitude of the analytical signal. The only assumptions made are uniform magnetization and that the cross section of all causative bodies can be represented by polygons of finite or infinite depth extent. This function and its derivatives are therefore independent of strike, dip, magnetic declination, inclination and remanent magnetism (Debeglia and Corpel, 1997).The 3-D analytical signal, A, of a potential field anomaly can be defined (Nabighian, 1984) as:

$$A(x,y) = \left(\frac{\partial M}{\partial x}\right) x + \left(\frac{\partial M}{\partial y}\right) \hat{y} + \left(\frac{\partial M}{\partial z}\right) \hat{z} \quad 3.3$$

Where M is the magnetic field

The analytical signal amplitude can now be calculated (Debeglia &Corpel, 1997) as:

$$|\,A(x,y)| = \sqrt{\left(\frac{\partial M}{\partial x}\right)\hat{x}^2 + \left(\frac{\partial M}{\partial y}\right)\hat{y}^2 + \left(\frac{\partial M}{\partial z}\right)\hat{z}^2} \qquad 3.4$$

3.5 Principles of Radioactivity

Radioactivity is the process in which an unstable atom becomes stable through the process of decay of its nucleus (Kearey *et al*., 2002). In the course of this decay, alpha (α), beta (β) and gamma (γ) rays are emitted. In radiometric survey, geologists and geophysicists measure the gamma rays emanating from the surface of the Earth. These radiations give a lot of information about the soil and rock distribution within the Earth *i.e* (lithology).

Radioactive elements decay to form isotopes. Isotopes are atoms of same element with equal number of protons but different neutron numbers. Isotopes have same chemical features, but different physical features. Unstable nuclei emit energetic ionizing radiations to become more stable. These isotopes are called radioactive isotopes or radioisotopes. Nuclides with this feature are called radionuclide, and disintegration or nuclear decay is the breakdown of unstable nuclei (IAEA, 2003).

Each radioactive isotope has a distinctive change associated with the radioactive disintegration of its nuclei. This is known as the isotope half-life and is the time taken for a radioactive nuclei to decay to half its initial value. Hence, after one half-life, half the original radioactive isotopes remain, and after two half-lives, one quarter of the original radioactive Isotopes remain, and so on (Minty, 1996). The law of radioactivity decay states that the reduction in the quantity of atoms of unstable nuclei with time is expressed as (IAEA, 2003):

$$N_t = N_o e^{-\lambda t} \qquad 3.5$$

Where N_t is the quantity of atoms after decay with time t(s),

N_o is the initial quantity of atoms and λ = the decay constant of the unstable nuclei (s^{-1}).

The half-life $T_{1/2}$ (s) of an element is defined as the time taken for N_0 to decrease by half. Half-lives vary 10^{-7}s for polonium-212 to about 10^{13}Ma for Lead-204 (Kearey *et al*., 2002).

$$T_{1/2} = 0.693/\lambda \qquad 3.6$$

The λ multiplied by N gives the activity of the unstable nuclei. Disintegration of unstable nucleus does not depend on additional physical factors (IAEA, 2003). Minty (1996) indicated that radioactivity usually occurs as a sequence of the number of daughter products with a breakdown of the mother elements in order to have a stable isotope. At this period, the behaviours of all the radioisotopes of the decay series are the same. Hence, the extent of the quantity of any daughter nuclei can be helpful in estimating the quantity of any other radio nuclei in the breakdown series. Emanations of gamma rays from the Earth surface differ with many factors but most importantly depend on the amount of radio nuclides in the top soil about 30 to 40 cm. The amount depends on the parent rock and the extent of weathering (Elawadi et al., 2004).

Table 3.1: Radioactive minerals (Telford, 1990)

RADIO ACTIVE ELEMENTS	MINERALS	OCCURRENCE
Potassium	(i) Orthoclase and Microline Feldspar ($KAlSi_3O_8$)	(i) Main constituents in acid igneous rocks and pegmatites.
	(ii) Muscovite [$H_2KAl(SiO_4)_3$]	(ii) Shale
	(iii) Alunite [$K_2Al_6(OH)_{12}SO_4$]	(iii) Alteration in acid volcani
	(iv)Sylvite,Carnallite [$KCl,MgCl_2.6H_2O$]	(iv) Saline deposits in Sediments
Thorium	(i) Monazite [ThO_2 + rare earth phosphate]	(i)Granites, Pegmatites, Gneiss.
	(ii) Thorianite [$(Th,U)O_2$].	(ii) Granites, Pegmatites, placers.
	(iii) Thorite, Uranothorite[$ThSiO_4$ + U].	(iii) Shale
Uranium	(i) Uraninite [Oxide of U, Pb, Ra+ Th, rareearth]	(i) Granites, pegmatites and with vein deposits of Ag, Pb, Cu, etc
	(ii) Carnotite [$K_2O,2UO_3.V_2O_5.2H_2O$]	(ii) Sandstones.
	(iii) Gummite [Uraninite alterations]	(iii) Associated with Uraninite

3.5.1 Radioactivity of rocks and minerals

All rocks and other earth materials are radioactive. Radiometry studies the distribution of radioactive material on earth, taking cognizance of the gamma radiations emitted by nuclear decay. Therefore, radiometry comprises of detecting nuclear emissions from rocks containing radioactive materials.

The uranium and thorium in igneous rocks is concentrated much in a few accessory minerals such as zircon, sphene and apitite (Slagstad, 2008). Other highly radioactive

minerals, such as monazite, allanite, uraninite, thorite, and pyrochlore, are widespread in nature but are very minor constituents of rocks, and are spread evenly. The host minerals of uranium and thorium are generally associated with felsic intrusions – particularly with younger intrusions; they can be located much less frequently in mafic rocks or in volcanics. The uranium and thorium content of rocks generally increases with acidity, with the highest concentrations located in pegmatics, (Slagstad, 2008). The highest concentrations of uranium and thorium in sedimentary rocks are generally found in shales.

For potassium in mostly concentrated in micas and feldspars; rocks with none of these minerals have very low potassium. Therefore, K-activity is very low in all mafic and ultramafic rocks. The potassium substance of sedimentary rocks is highly variable but tend to be higher in shale than in carbonates or sandstones.

3.5.2 Ratio radioelement maps

A ternary radioelement map is a colour composite image generated by modulating the red, green and blue phosphors of the display device or yellow, magenta and cyan dyes of a printer in proportion to the radioelement concentration values of the K, Th, U and TC grids. The use of red, green and blue for K, Th and U respectively, is standard for displaying gamma ray spectrometric data. Blue is used to display the U channel, since this is the noisiest channel and the human eye is least sensitive to variations in blue intensity. Areas of low radioactivity and consequently low signal to noise ratios can be masked by setting a threshold on the total count grid. This reserves more colour space and ensures a better colour enhancement for the remaining data.

Sum-normalization can be used to compute relative concentrations of K, Th and U prior to imaging as follows:

Kn = K/ K+U+Th

Un = U/ K+U+Th

Thn = Th/ K+U+Th

This converts the radioelement concentrations to relative abundance.

3.5.3 Radiometric anomalies

Geological information is the basic key to the interpretation of all radiometric data collected in the field (Uwah, 1984). The purpose of initial reconnaissance is to decide whether it is worthwhile to make a systematic gamma ray survey of the area in question (Uwah, 1984).The three principal natural radioactive elements of the earth crust are potassium (K-40), uranium (U-238) and thorium (Th-232). The most abundant of the three is K, found mainly in alkali feldspar, mica, neptheline and leucites (Galbraith and Saunders; 1983). Most crustal rocks contain at least in trace quantities, the three radioactive elements. Since changes in radioactivity level are reflections on radioisotope contents of the rock (and hence, geological contact), it is possible for correlation to be made between radioactivity of an area and rock types (Galbraith and Saunders, 1983). Such correlation is however seriously affected by the presence or absence of soil and also by the type of soil. Radioactivity of the bedrock is reflected only if the bedrock is exposed or has very thin overburden of few centimetres. The characteristic of a great majority of economic uranium deposits is the preferential enrichment of uranium relative to thorium and potassium. This preferential enrichment may exceed the relative abundance found in normal rock by several orders of magnitude (Darnley, 1973).

For any radioelement to be extracted economically, they have to be located where they have already been concentrated by geological processes. According to Darnley (1972) this must be about 250 times the average content in normal rock and in addition their ratios must reflect preferential enrichment of the particular element to the other (Uwah,

1984). Most radiometric anomalies require thorough investigations before conclusions are made as to their economic importance (IAEA, 1991).

CHAPTER FOUR

4.0 RESULTS AND DISCUSSION

4.1 Residual Magnetic Intensity Map (RMI)

The residual magnetic intensity map (Figure 4.1) produced shows areas of varying colours which connotes regions with rocks of different magnetic susceptibilities and also corresponding to different lithologies and depth of source rock. The map exhibits both positive and negative magnetic anomalies ranging from -25.0 to 110.7nT. The areas with pink and red colour depicts rocks with positive anomalies while green to blue depicts negative anomalies. Changes in magnetic signature from high to low and vice versa were observed in the map. The high magnetic signature occupies mostly the North-eastern and South-western region of the map while the South-eastern and North-western region have low magnetic signatures. The amplitude of a magnetic anomaly depends on the magnetic susceptibility of the rocks at specific geographical locations. The south-eastern part of the map with low magnetic signatures depicts the sedimentary rock region which corresponds with the Lafia sandstone as well as the alluvial deposits. This tallies with what was obtained from the geology map of the area. The low magnetic signature at the south-eastern part of the map may be attributed to low magnetic minerals in the sedimentary rock. The central portion of the map also has low magnetic signature which coincides with the migmatite in the geology map. The migmatites showed low magnetic susceptibility because the parent rock (protolith) is of sedimentary origin which has low magnetic susceptibility.

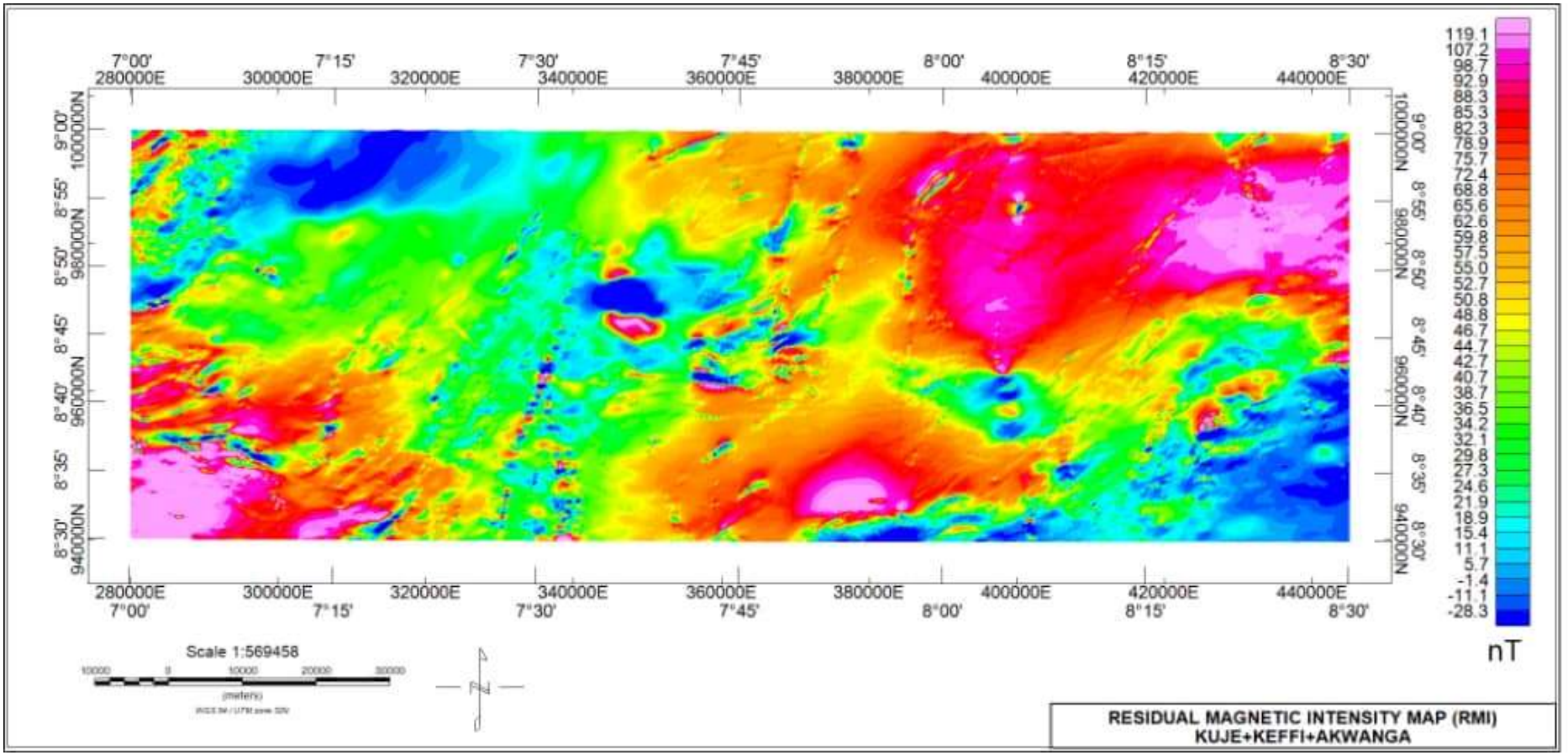

Figure 4.1: Residual Magnetic Intensity Map of the Study Area

4.2 RMI Reduce to Equator (RTE) Map

The RMI data was reduced to equator by assuming an inclination (I) equal to -7.25 and a declination (D) of -1.97 according to IGRF (International Geomagnetic Reference Field) .The RTE map helps to remove the effect of magnetic inclination in regions with low latitude by centring the peaks of magnetic anomalies over their sources.

The extreme south-eastern region of the map has low magnetic frequency which is an indication that it is a sedimentary region. The north-central area which shows greenish colouration has a relative weak magnetic signature which extends towards the north-western area. The negative magnetic anomaly is as a result of weathered basement. Figure 4.2 shows the RMI map reduced to equator.

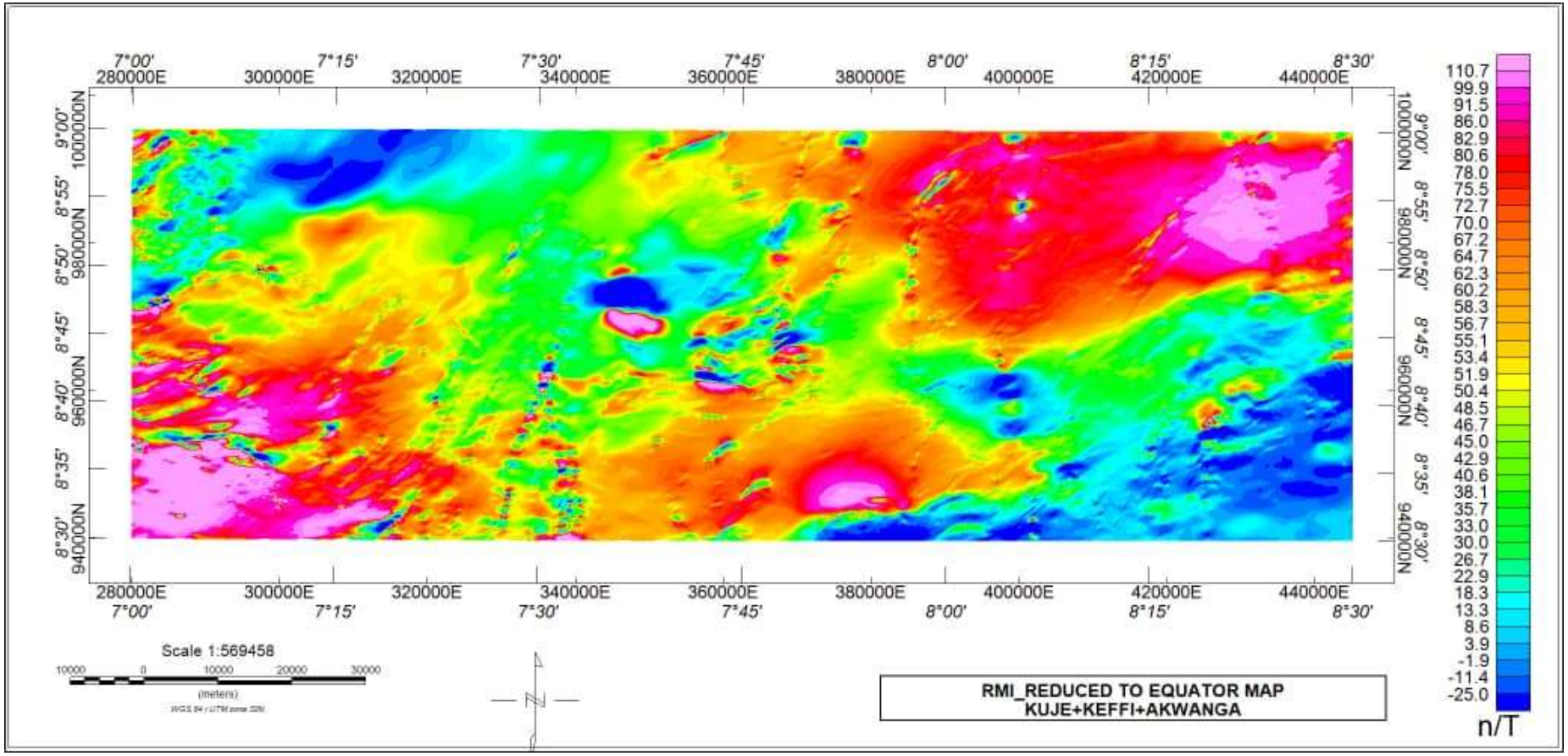

Figure 4.2: Residual Magnetic Intensity Map Reduced To Equator.

4.3 RMI Reduce to Pole (RTP)

The RTP map in Figure 4.3 shows high and low magnetization. The magnetic susceptibility ranges from -119.1255 to 28.4702 nT/m. The map revealed that the south-eastern area of the map has positive anomaly which indicates high magnetic susceptibility. The extreme north-western and north-central part of the map also show high magnetic susceptibility with some little patches showing low susceptibility. On the other hand, the north-eastern, south-western and south-central region of the map revealed rocks with low susceptibility.

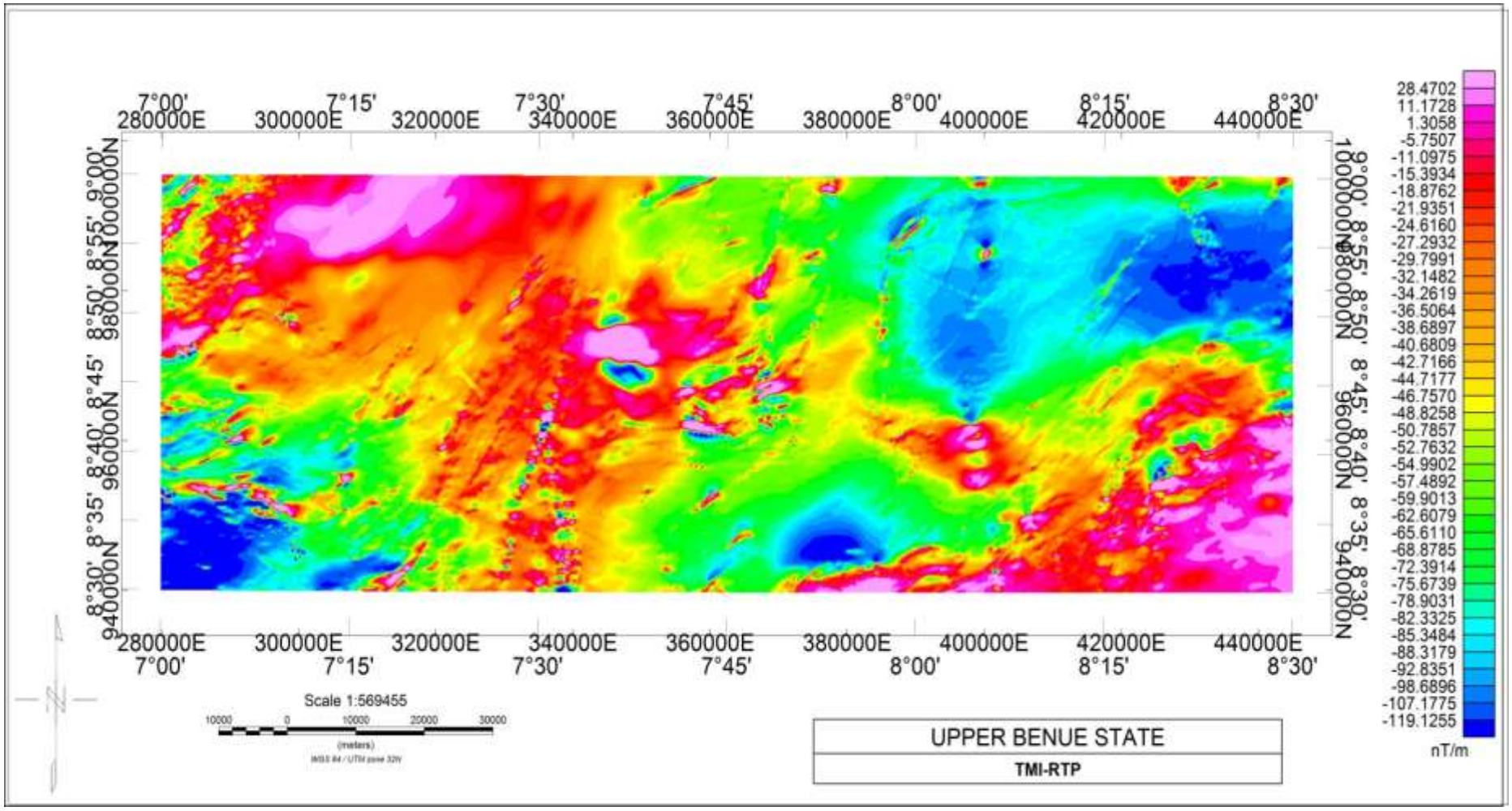

Figure 4.3: TMI Reduced to Pole

4.4 Horizontal Derivatives (HD)

The map of the horizontal gradients of total magnetic intensity along the x and y direction (Figures 4.4 and 4.5 respectively) represents the rate of change of the magnetic field in the y and x directional axes by highlighting the anomalies with high components disposed along the both axes. The horizontal derivatives in both directions (Δx and Δy) are denoted by Δz (Figure 4.6).

The SW and extreme NW region are dominated by highly distorted short wavelength magnetic signatures. Also the highly distorted signatures can be seen scattered in small fragments in the North-central and South-eastern area of the map. These short wavelengths of magnetic signatures are characteristic of outcrops and shallow intrusive magnetic bodies that are weathered. The extreme South-eastern part characterized by long wavelength signatures is an indication of area with thick sedimentation. The north-eastern part of the study area is mixed with long and short wavelength which also extends towards the south-central region is an indication of sedimentation with scattered patches of outcrops.

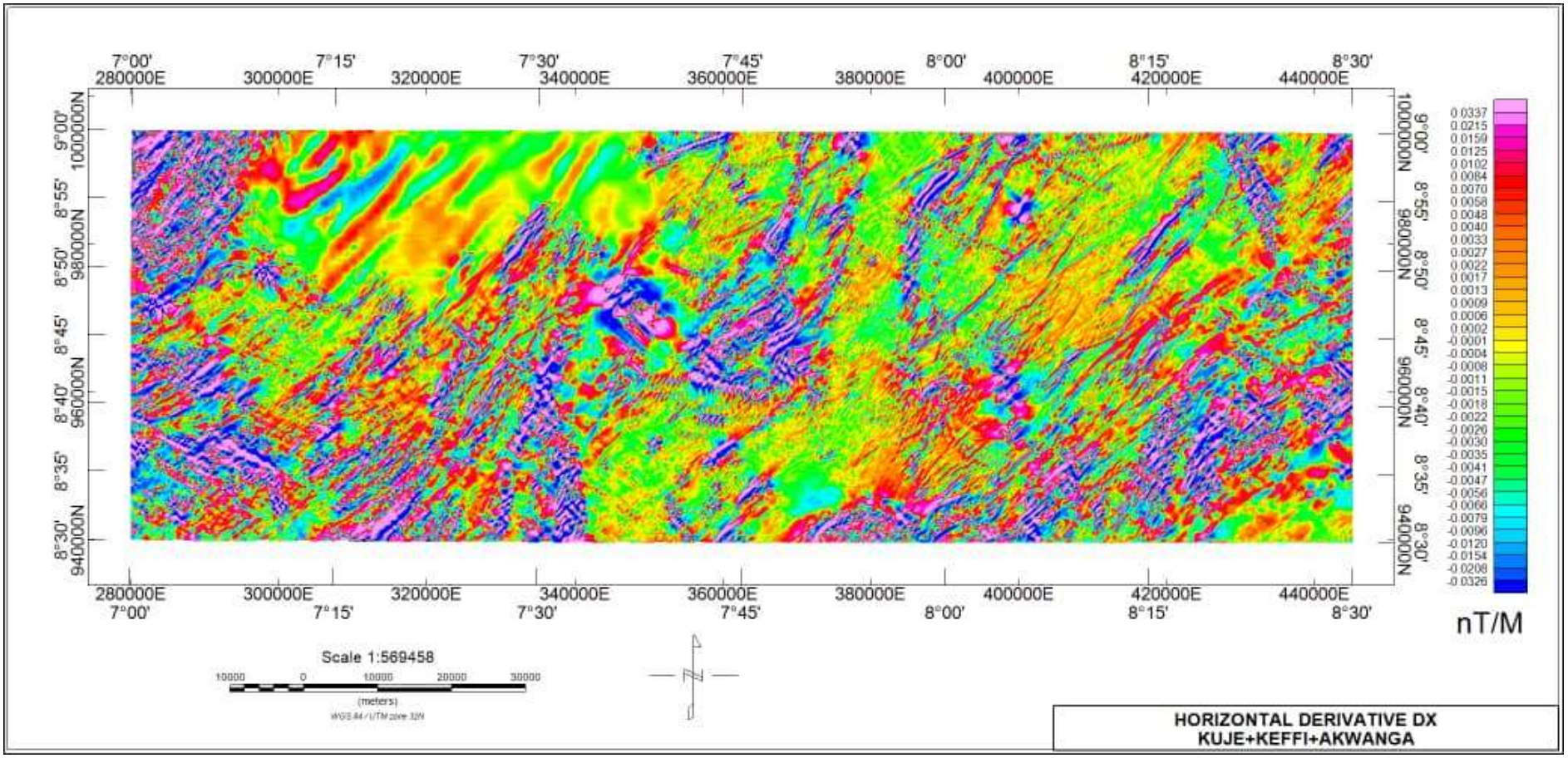

Figure 4.4: Horizontal Derivatives Map (HDx) of The Study Area

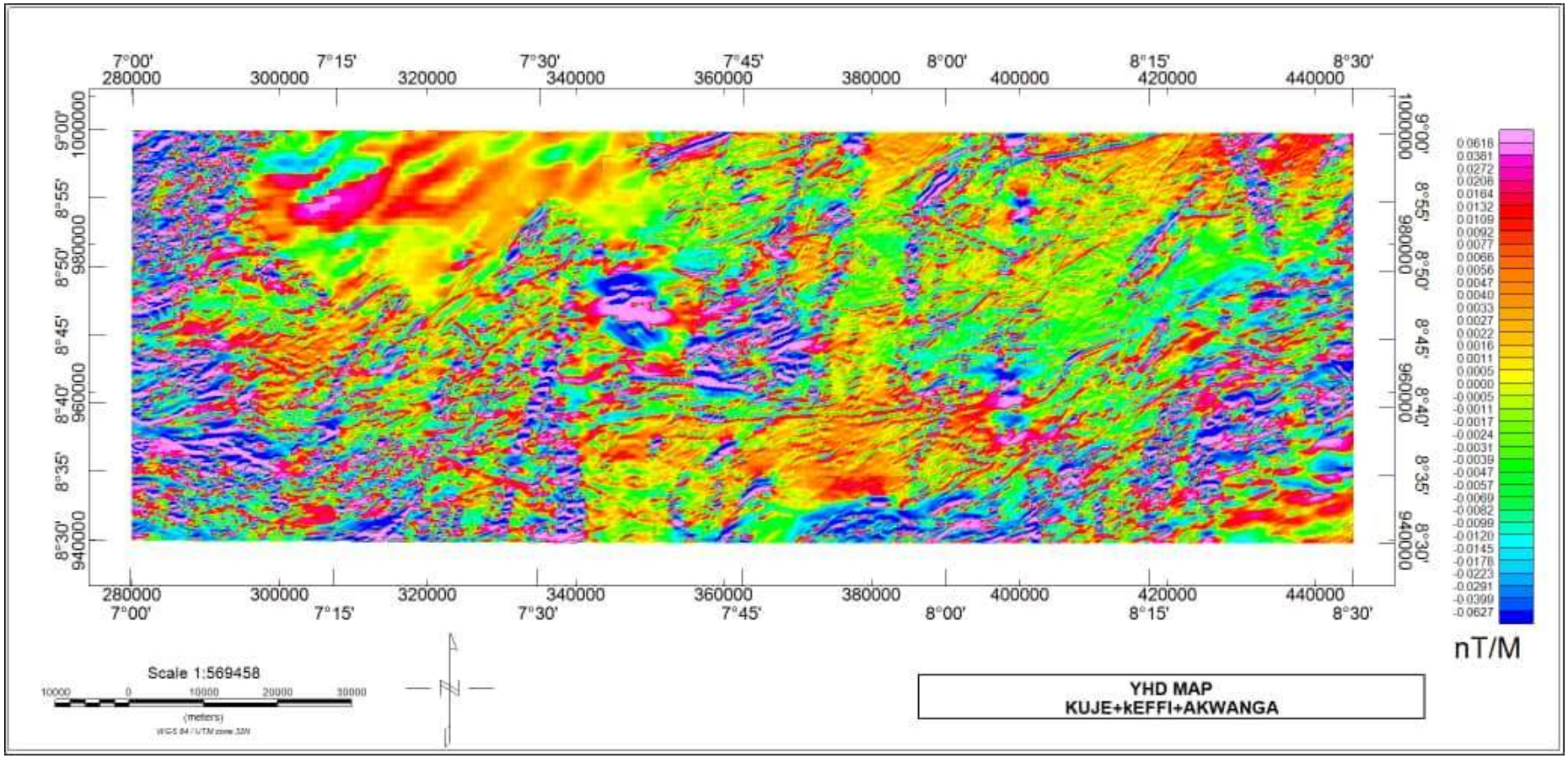

Figure 4.5: Horizontal Derivative (HDy) of The Study Area.

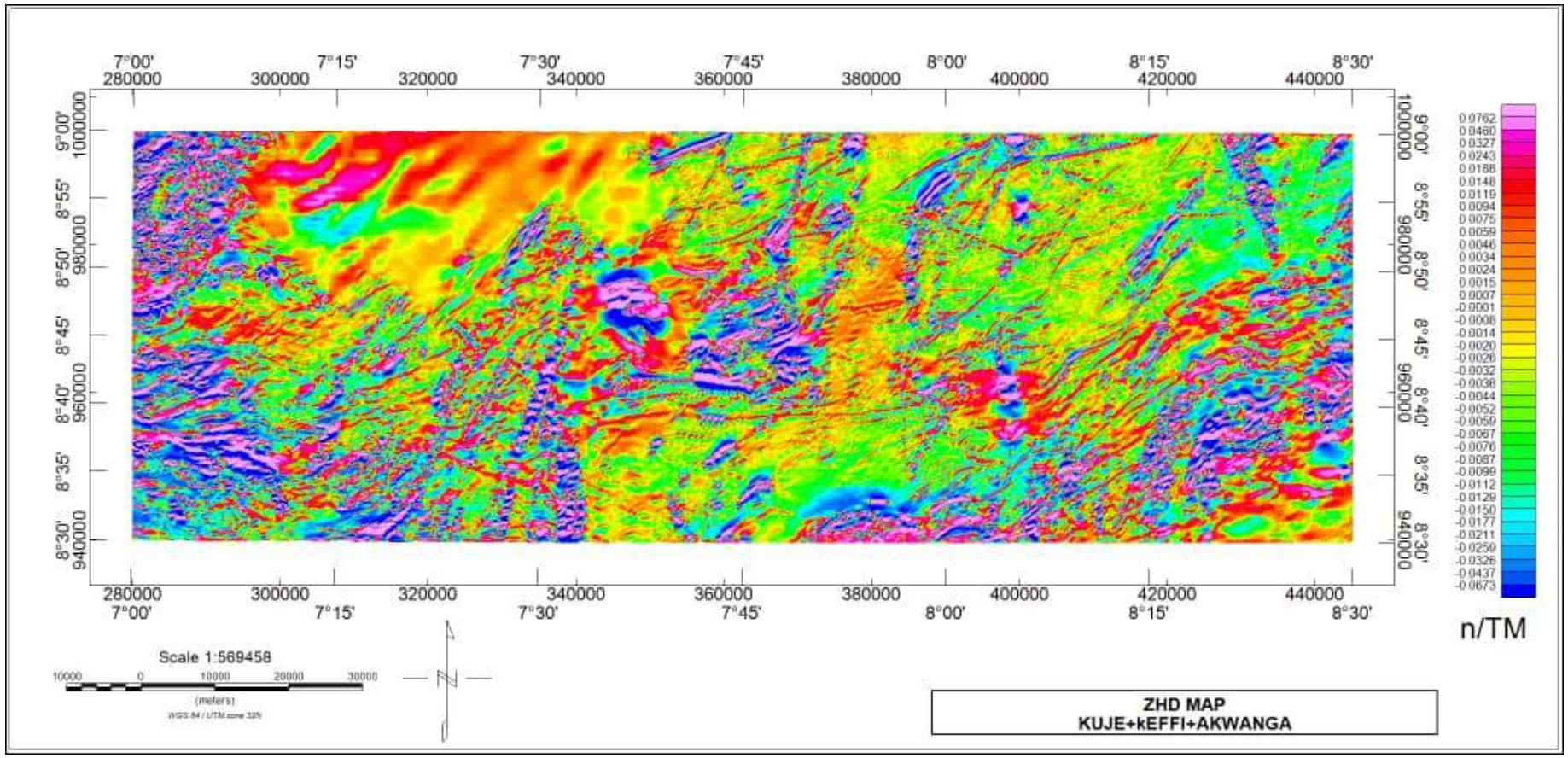

Figure 4.6: Horizontal Derivative Map (HDz) of The Study Area.

4.5 First Vertical Derivative Map (FVD)

The first vertical derivatives (Figure 4.7) enhances near surface features such as faults, folds and lineaments .The vertical derivative map is much more responsive to local influence than to broad or regional effects and therefore tends to give sharper picture than the Residual Magnetic Intensity map. One of the important applications of first vertical derivatives is finding magnetic lineaments and determining the boundary between lithological units more precisely.

In the coloured aggregate map, pockets of intrusions were seen around the central and south-eastern portion of the map. Migmatite, migmatite-gneiss and biotite-gneiss are the main basement that were intruded. The features that could be interpreted from the map include: intrusive bodies, faults, lineaments and fold. The portion labelled A1 coincides with the region of porphyritic granite; A2 undifferentiated granite and muscovite schist, while A3 and A4 falls within the region of biotite granite intrusions.

4.6 The First Vertical Derivative (Grey Scale Map)

The structural features in the FVD are clearer in the grey scale map (Figure 4.8). Fault lines were seen in the western and eastern end of the map. Many lineaments were seen but the prominent ones were mapped. Worthy of note is a long stretch of lineament towards the south-west region located at Latitude 8.30^0N-8.50^oN and Longitude 7.24^oE-7.25^oE. Another prominent lineament was mapped towards the north-eastern area of the map which terminated at a thin patch of an intrusive rock corresponding to the medium to coarse grained biotite-granite .These lineaments trend in the northeast-southwest direction while the fault lines trend mostly northeast-southwest and east-west directions. Also clearly seen in the map are folds. These folds were clearly mapped out and one of the folds was seen to occur at the contact between the sedimentary rock and the basement. The other folds were found in the areas of intrusion, denoted as A3 and A4.

These folds in A3 and A4 were as a result of intrusions of magma in the rock, forcing the overlying rock to arch up.

Finally, towards the north-western region of the map marked in black curve in the grey map and which lies between Longitudes 7.10^{o}E - 7.37^{o}E and Latitude 8.47^{o}N – 9.00^{o}N is an interpolated data. There was no interpretation on the data because it did not give the true picture of the geology of the area.

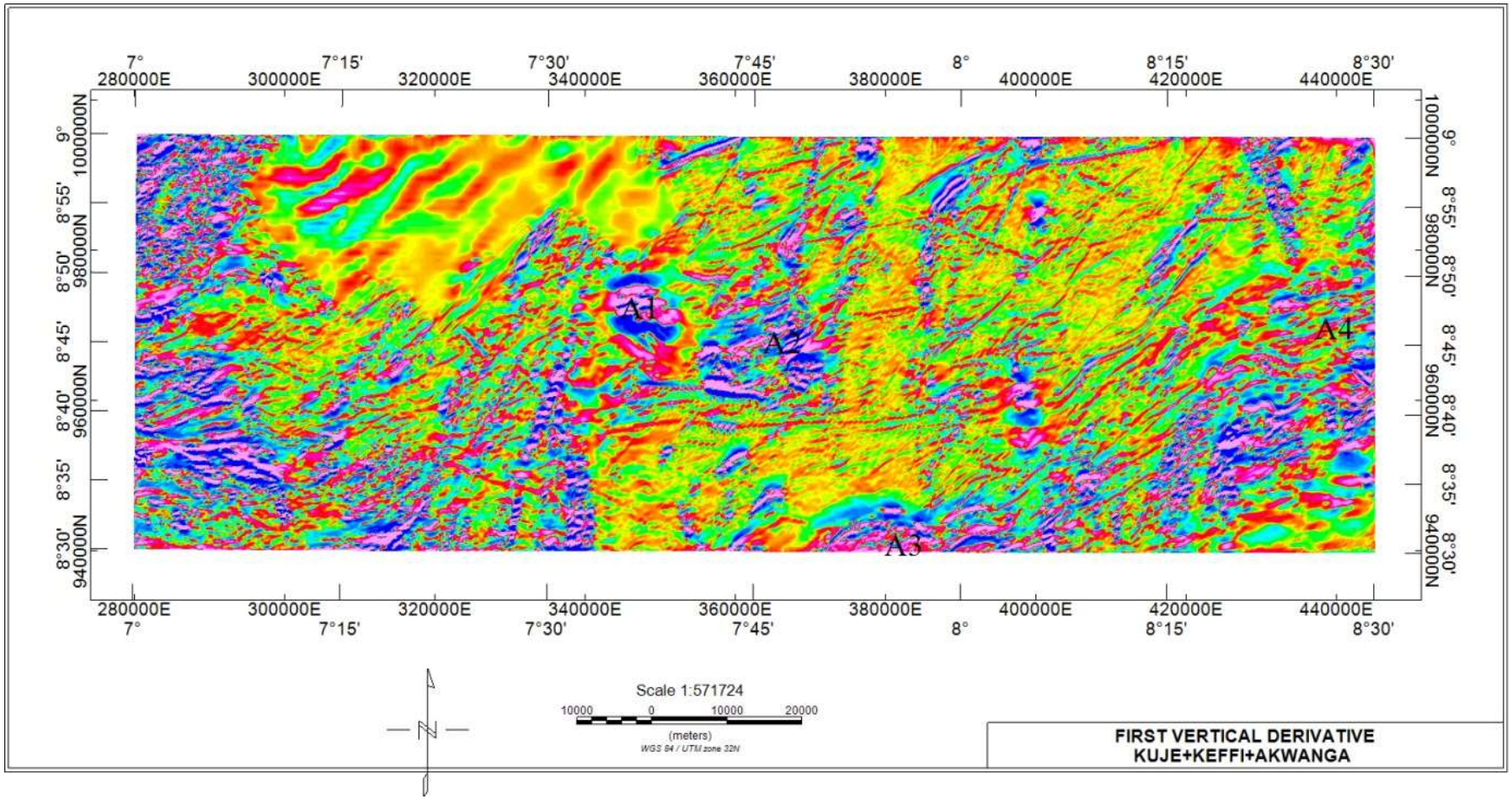

Figure 4.7: First Vertical Derivative Map (coloured)

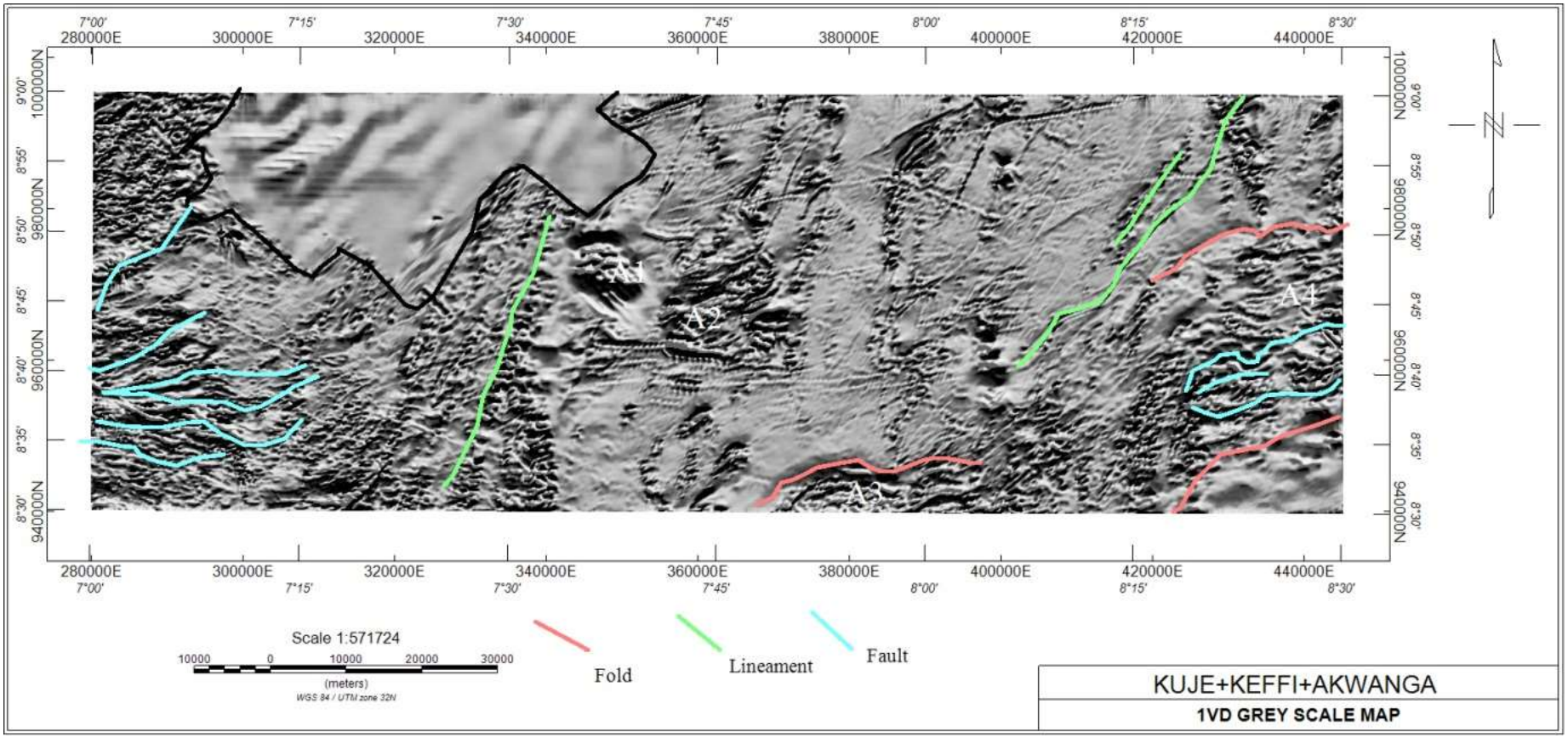

Figure 4.8: First vertical derivative map (Grey Scale)

4.7 Analytical Signal (AS)

The analytical signal filter represents the magnetic anomaly of the causative body which depends on the location of the body (horizontal coordinate and depth) and devoid of its magnetization direction.

The analytical signal map is to be interpreted in terms of susceptibility of rocks relative to the geology map, thus bodies with high susceptibility appearing as isolated spherical or round shapes are various granitic bodies that are separated by their degree of magnetisation in consonance with susceptibility. The 3-D analytical signal map (Figure 4.9), shows a susceptibility range of 0.0039 – 0.1550 nT/m was observed.

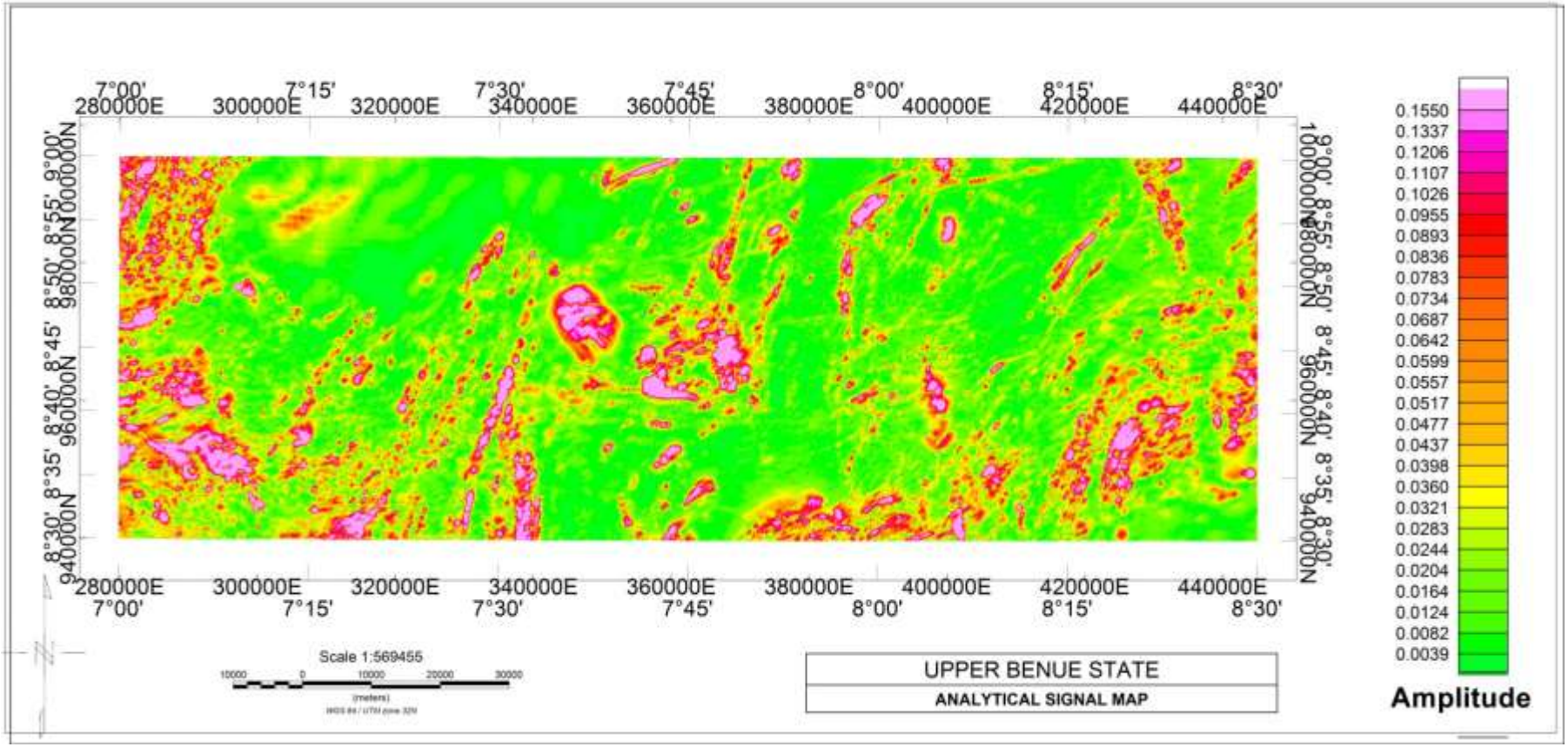

Figure 4.9: Analytical Signal Map of The Study Area

4.8 Potassium (K), Thorium (Th) and Uranium (U) Concentration Maps

The concentration map can be used to depict the lithology of the rock formation in the study area. The potassium concentration is expressed in percentage (K%), that of Thorium in parts per million (ppm) and also that of uranium in parts per million (ppm).

The K concentration map (Figure 4.10) shows that the extreme South-eastern and South-western end of the map which is made up of sandstone and undifferentiated schist rocks respectively have low concentration of Potassium of between 0.3 - 0.8% while the areas that have moderate concentration (0.8 - 1.6%) are mostly underlain by migmatite. The lineament located at longitude 7.30^{o}E is enriched with potassium. All the intrusions labelled A1, A2, A3 and A4 in the FVD map along with other patches of intrusive rocks have high potassium concentration. Also worthy of note is the faulted region in the western end of the map which has low to moderate level of concentration of potassium. Moreover it was seen that the granitic rocks have the highest concentration of Potassium ranging from 1.6 - 4.1%.

Similarly,in the thorium concentration map (Figure 4.11), the sedimentary region which consists mostly of sandstone has the lowest concentration level of thorium which falls in the range of 7.9 - 11.6 ppm. The intrusive bodies mapped A1 and A2 in the FVD map has low thorium concentration. Also the elongated lineament located towards the western portion of the map has low thorium content.

Towards the central region of the map which has high predominance of migmatite rock is observed moderate concentration of thorium which ranges from 11.6 ppm - 14.9 ppm. Moreover, the faulted area in the western edge of the map has high concentration of thorium. The highest concentration level of Thorium which is 37.2 ppm is associated with mostly biotite-granite rocks.

In the same vein, the uranium map (Figure 4.12) shows that the highest level of uranium concentration is associated with the biotite granite which falls in the range 3.8 - 8.1ppm while the sedimentary region has the lowest ranging from 0.9 - 2.1 ppm. The elongated lineament which is located towards the western part of the map has low uranium concentration. The thin stripe of intrusive rock located towards the extreme north-eastern end has high uranium concentration while the intrusive body labelled A1 in the FVD map has low concentration of uranium. Also the intrusive body A2 has low to moderate level of concentration of uranium. The migmatite rock which dominates the central area of the map has moderate level of concentration (2.1-3.8 ppm). Furthermore, the faulted area in the western edge of the map has moderate level of concentration of uranium

The concentration maps when compared with the geology map of the area show near agreement. It can be seen from the concentration maps that the granitoids are the rocks with the highest concentration of the radioactive minerals. Also worthy of note is that the biotite-granite intrusions which are located towards the eastern end of the map at Longitude 8.20^{o}-8.30^{o} E and Latitude 8.44^{o}N- 8.50^{o}N and the south-central region of Longitude 7.46^{0}-8.04^{0}E and Latitude 8.30^{o} – 8.33^{o}N has all the three radioactive elements in high proportion while the sedimentary region has them in low amount.

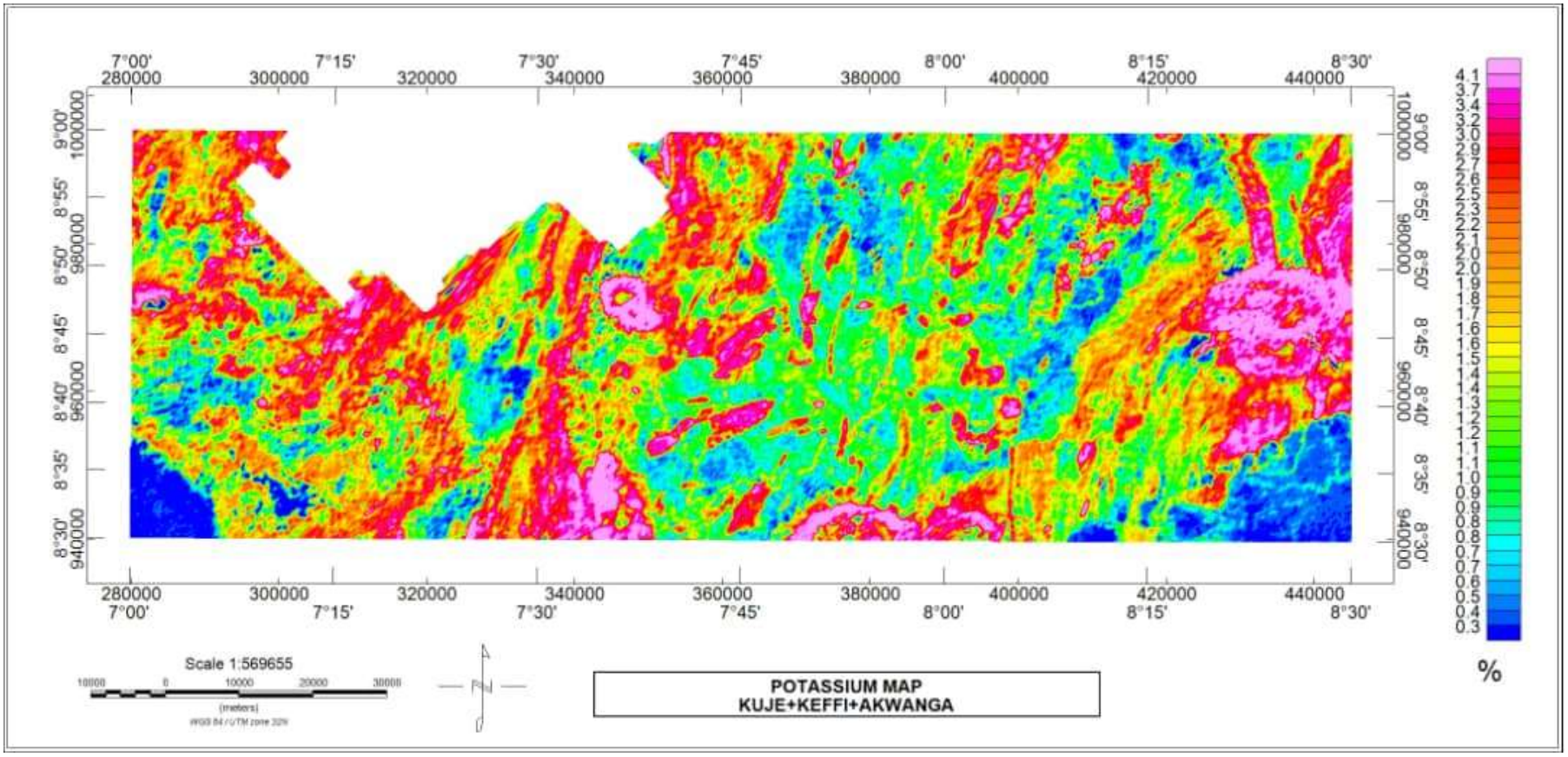

Figure 4.10: Potassium Concentration Map of The Study Area

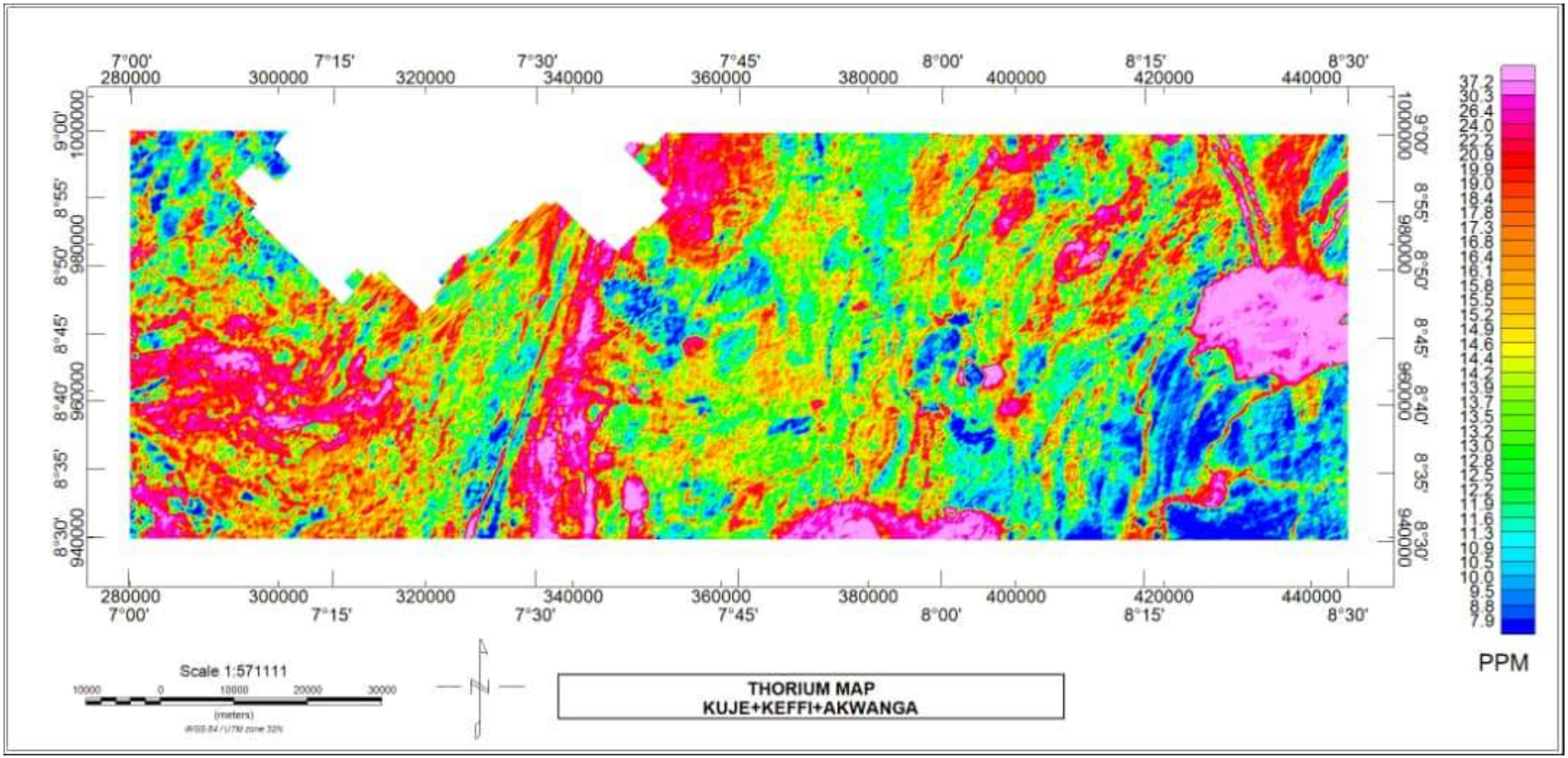

Figure 4.11: Thorium Concentration Map of The Study Area

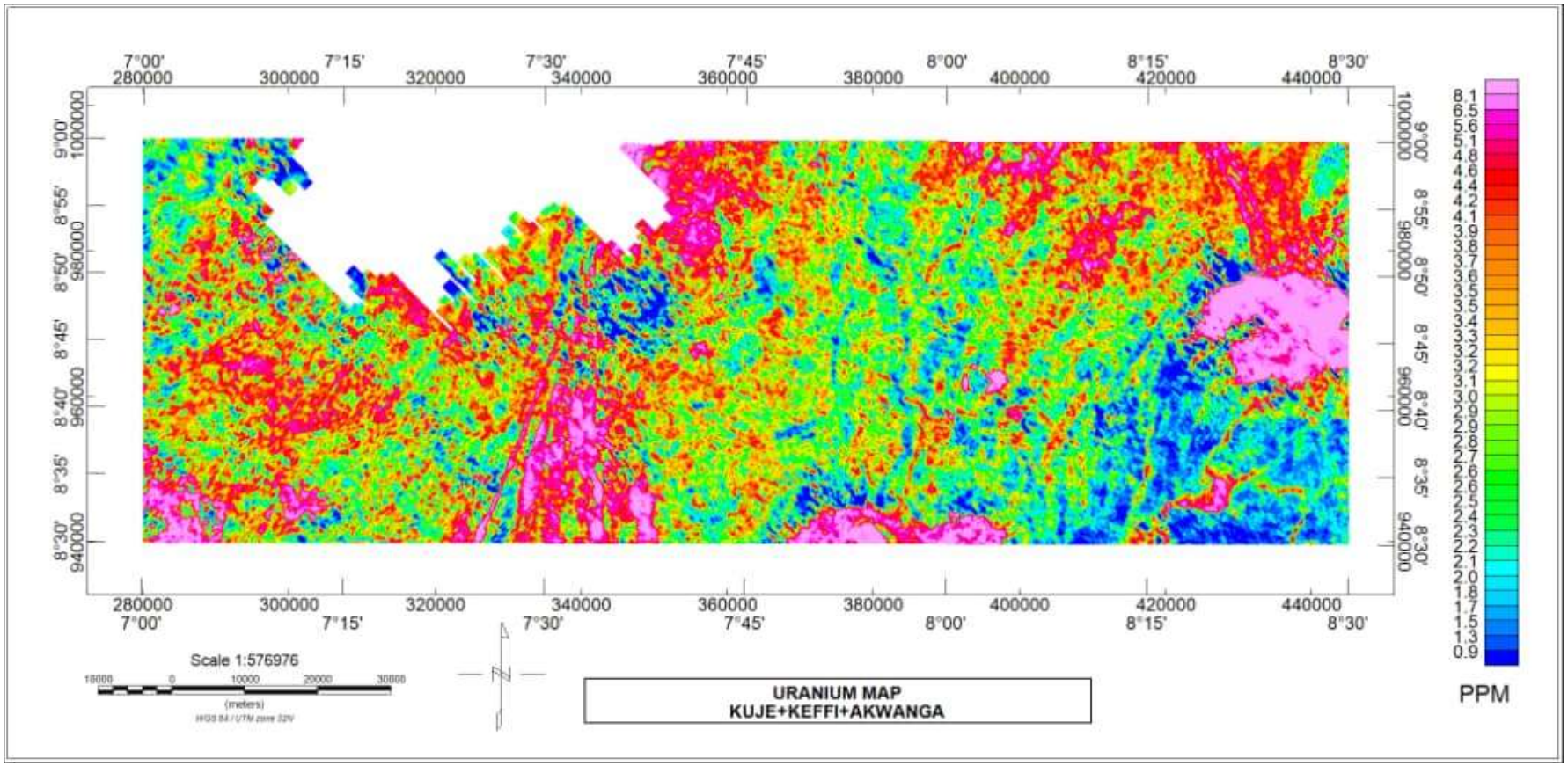

Figure 4.12: Uranium Concentration Map of The Study Area.

4.9 Ratio Map of K/Th , Th/K, K/U,U/Th and U/K.

Ratio maps show the enrichment or depletion of a particular radioelement over another. Therefore they are useful in delineating regions of hydrothermal alteration. Potassium concentration is expressed as a percentage (K%) ; thorium as equivalent thorium (eTh) and uranium as equivalent uranium (eU) .Thorium (Th) is typically regarded as immobile in the process of mineralization, but it can be partly depleted in areas of intense potassium (K) alteration. In other words, K/eTh is a better indicator of hydrothermal alteration than any single radio-element alone.

In many gold deposits, Th has been mobilized and depleted with the resultant increase of K (Hoover *et al*,1992, Dickson and Scott ,1997 and Durrance,1986). The K/eTh ratio map shows that high content of Potassium which is denoted with red colour implies low content of thorium and low content of potassium indicates high content of thorium. A constant ratio exists between potassium and thorium in most rocks typically varying from 0.17 to 0.2 K/eTh (in %/ppm) (Hoover *et al*, 1992); therefore rocks with K/eTh range outside this ratio are known as potassium or thorium specialized (Portnov, 1987). That is to say, rocks above this range are known as potassium-rich while those below the range are termed thorium-rich. Therefore the rocks which show high K/Th ratio value are the strong indicators of hydrothermal alteration.

From the K/eTh map in Figure 4.13, the areas dotted with the pink colours have high value of about 0.3 %/ppm of K/eTh ratio which is above the stated benchmark and therefore indicates region of hydrothermal alteration. Another interesting feature that cannot be ignored is the potassium enrichment of the medium to coarse grained biotite granite that shared boundary with the sedimentary rock in the extreme south-east area of the map. The same rock type (biotite granite) with different texture and located at Latitude 8.44^{o}N-8.50^{o}N and Longitude 8.20^{o} – 8.30^{o}E also has a boundary with the

medium to coarse-grained biotite granite; but the biotite granite has equal ratio of K/eTh while the medium to coarse-grained rock has high K/eTh ratio. This is because, hydrothermal fluids might have flowed through the fractured rocks thereby enriching it with potassium at the expense of thorium. Also worthy to note is the high K/eTh ratio of the elongated lineament located towards the western area of the map. This is another region of hydrothermal alteration. This is because the surrounding migmatite rock through which the lineament passed through has approximately equal K/eTh ratio, therefore some hot aqueous mineral-laden fluids might have flowed through the lineaments thereby depleting thorium. These regions described as alteration zones correspond to areas with fractures in the First Vertical Derivative map. This suggests likely area of gold mineral deposits because gold forms in an area of intense potassium alteration.

Also, the intrusion labelled A1 and A2 in the FVD along with most minor intrusions show high K/Th ratio and the ones mapped A3 and A4 have equal ratio of K/Th. An interesting feature was observed in the western region of the map and that is a reddish curved stripe. The reddish curved band delineates change in lithology. This feature was also found in the potassium concentration map. The extreme south-western end of the map shows the lowest K/Th ratio an indication that the region has no potassium content.

The Th/ K (Figure 4.14) is the reverse of the K/Th ratio map in the sense that regions with high Thorium content are regions with low Potassium content and vice versa in the K/Th ratio map.

The K/U map in Figure 4.15 is similar to the K/Th map. It shows the areas of enrichment of K at the expense of U. Uranium is unstable and can easily be mobilized, therefore K/U ratio are not usually used to delineate regions of hydrothermal alteration. However, K/U ratio can serve as a useful tool to delineate contacts or geological

boundary. In the K/U map , a distinct boundary could be seen between the basement and the sedimentary rocks. Also the curved reddish band observed in the K/Th map was also seen in the K/U map and this feature delineates lithological change.

On the other hand, the eU/eTh ratio map (Figure 4.16) depicts the ratio of equivalent uranium (eU) concentration to equivalent thorium (eTh). Thorium is more stable than uranium hence the predominance of low eU/eTh ratio in the map. Most of the intrusive rocks also have low U/Th ratio of which the most pronounced is the intrusive labelled A1 in the FVD map. Also the sedimentary region, extreme north-eastern region and some areas in the central and the western part of the map have low eU/eTh ratio. The regions with high eU/eTh ratio include: the extreme south-west, the immediate surrounding areas of the longest lineament towards the south-west, the intrusion A1 and some parts of the north-eastern end of the map. The biotite granite intrusions at Latitude 8.43^{o}N-8.46^{o}N and Longitude 8.20^{o}E-8.30^{o}E and that located at Longitude 7.46^{o}E-8.04^{0}E and Latitude 8.30^{o}N- 8.34^{o} N have equal eU/eTh ratio.

The eU/K map (Figure 4.17) is the reverse of the K/eU map. Areas in the map with high K/eU ratio in the K/eU map shows low eU/K ratio in the eU/K map and areas with low K/eU ratio in the K/eU map shows high eU/K ratio in the eU/K map.

It can be seen from the eU/K map that the extreme south-western and south-eastern edge have relatively high eU/K ratio. The central portion of the map depicts rocks with equal and high eU/K ratio. The intrusion A1 and the elongated lineament close to it have low eU/K ratio.

The abundance ratios of K/eTh, K/eU, eU/K and eU/eTh are better indicators of changes in rock types, alteration or depositional environment than the value of the radio-isotopes themselves.

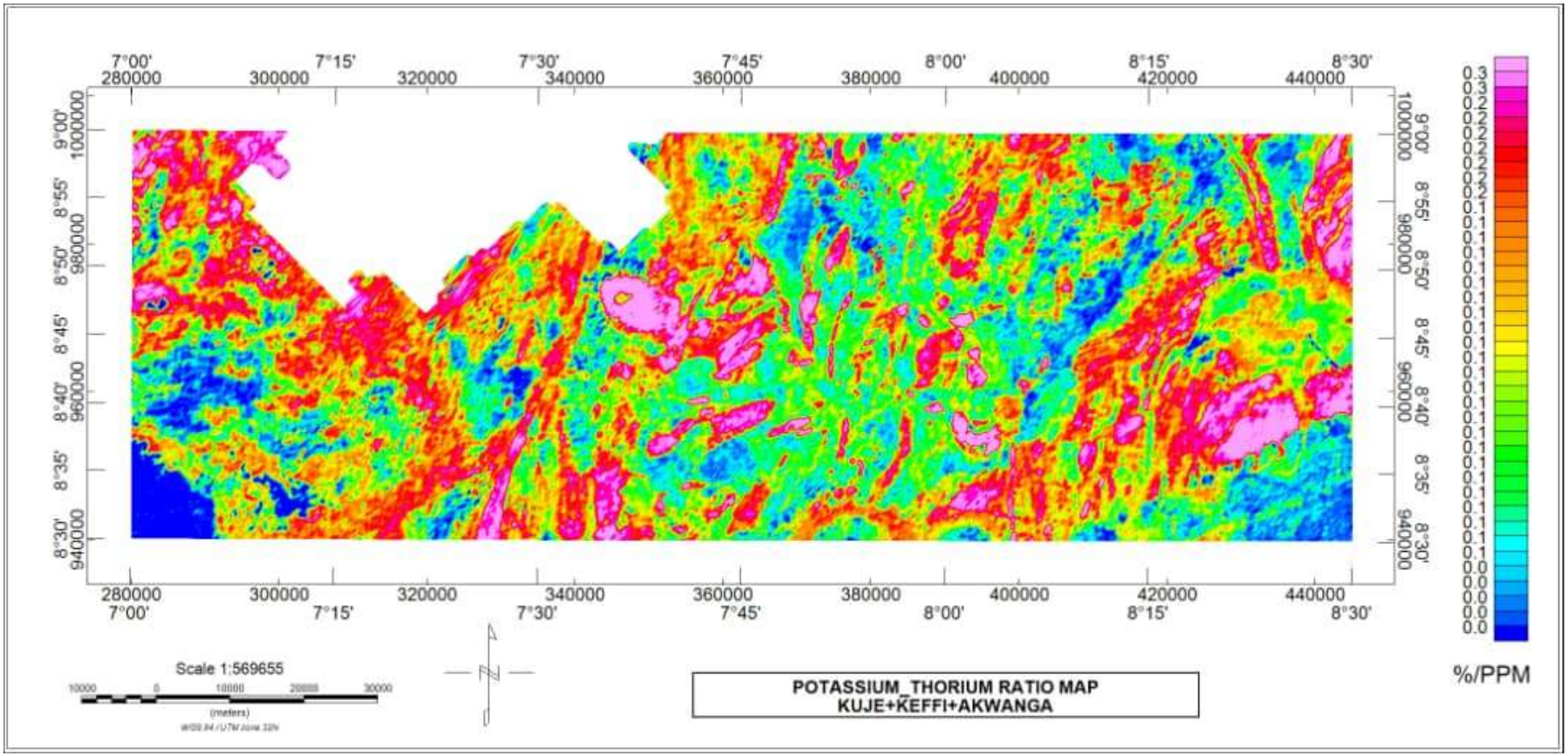

Figure 4.13: Potassium/Thorium Ratio Map

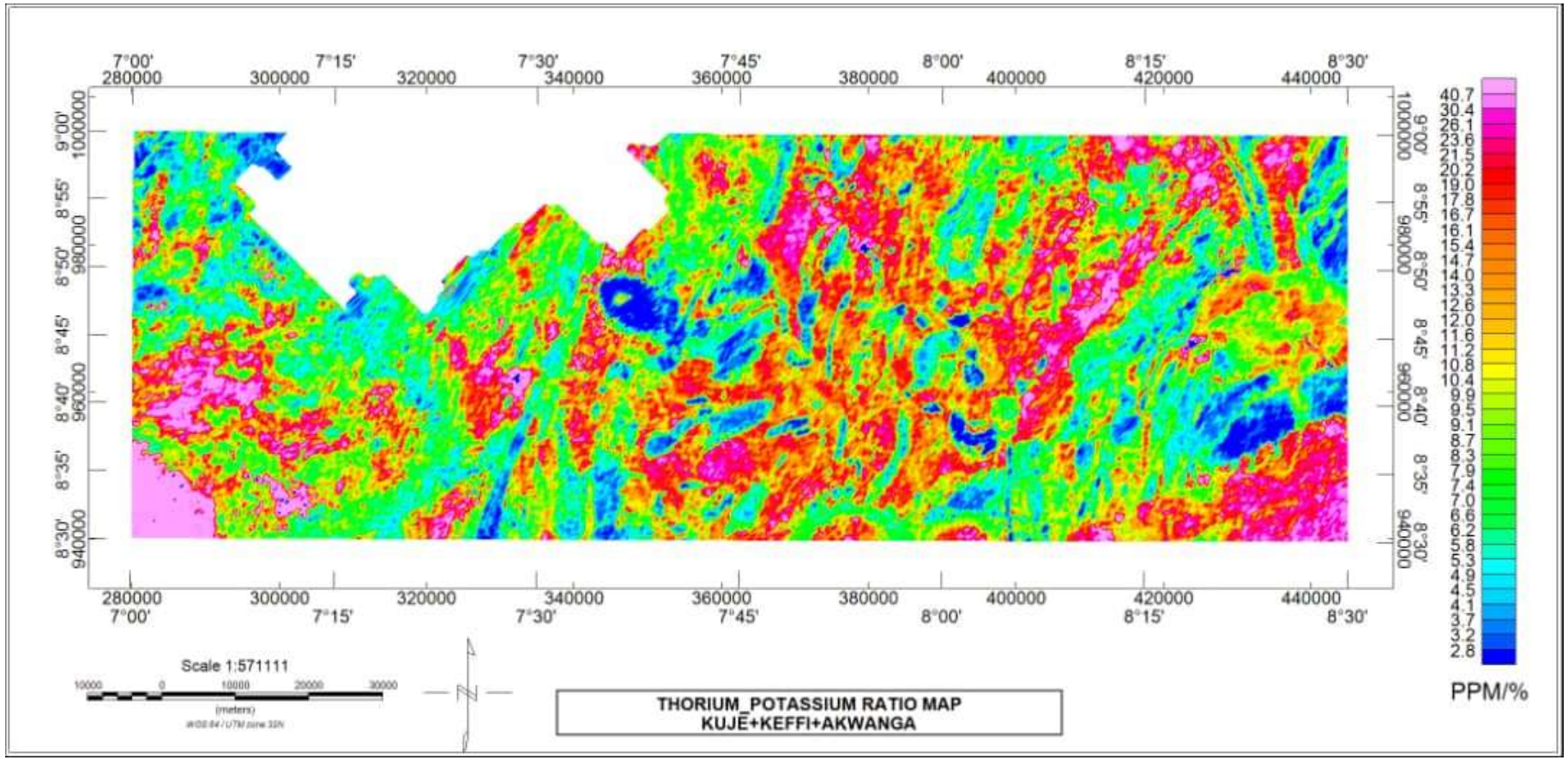

Figure 4.14: Thorium/Potassium Ratio Map.

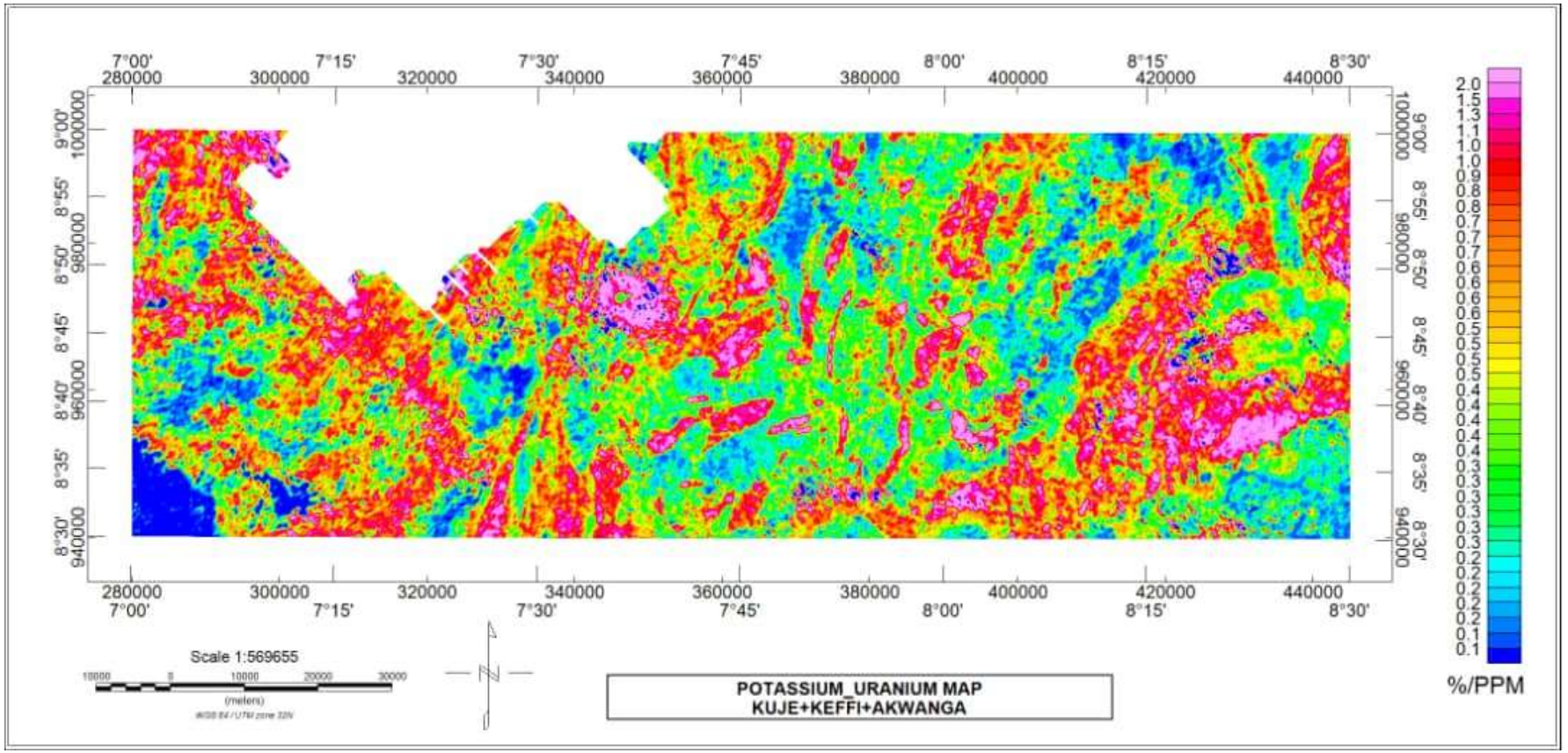

Figure 4.15: Potassium/Uranium Ratio Map

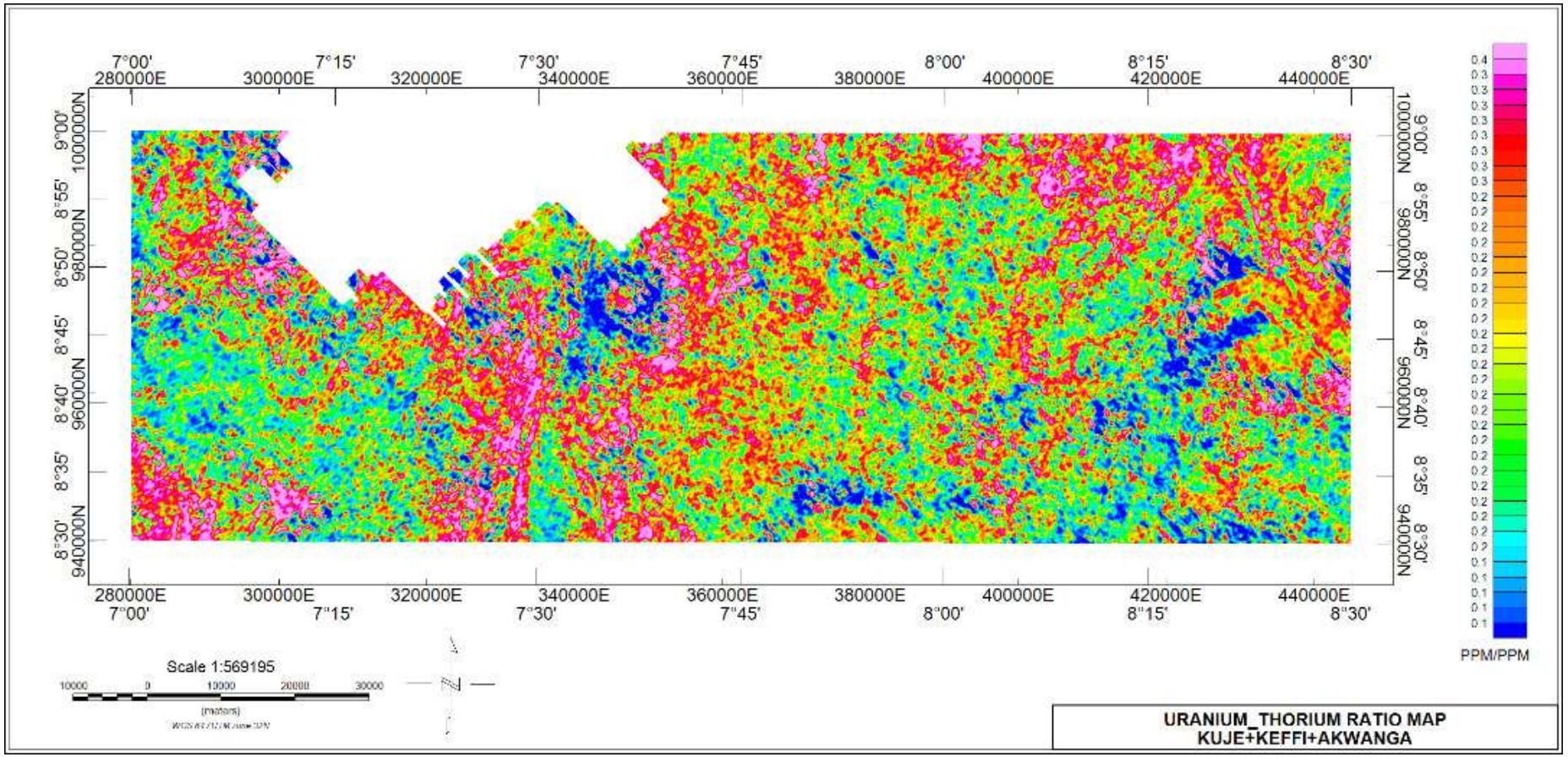

Figure 4.16: Uranium/Thorium Ratio Map

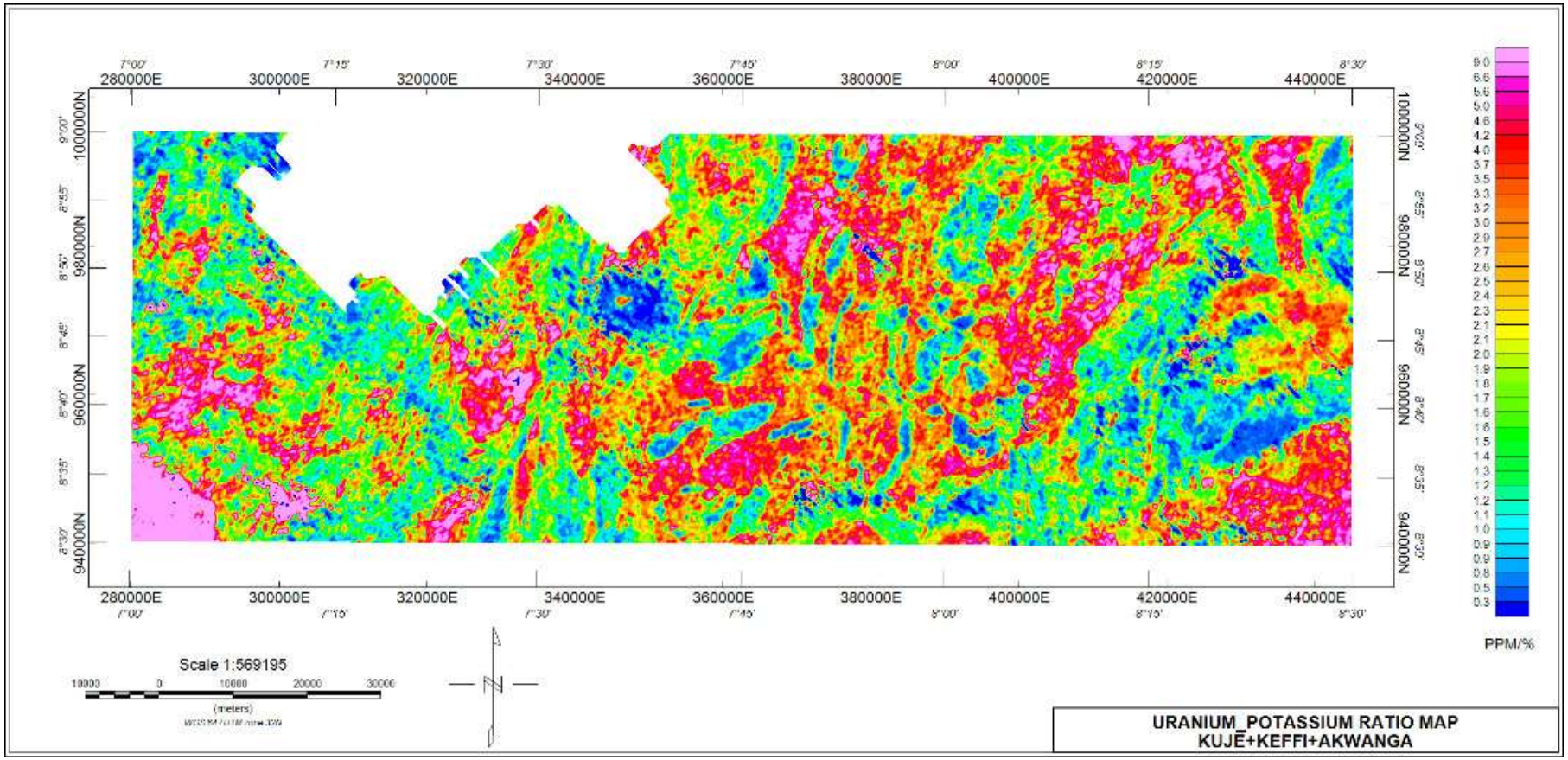

Figure 4.17: Uranium/Potassium ratio map.

4.10 Ternary Map

The ternary image (Figure 4.18) is a combination of colours produced from the individual concentration of colours produced from the individual concentration of the gamma radiations and corresponds to slight differences in the relative amounts of the three components. The blue colour represents relatively high uranium with low potassium and thorium. Red indicates high potassium with low uranium and thorium. The green colour shows high thorium with low K and U. The light blue colour (Cyan) denotes high thorium and uranium with low potassium. The brownish-red colour (magenta) shows high potassium and uranium but low thorium. Yellow is an indication of high potassium and thorium with low uranium. Black indicates low potassium, thorium and uranium while white indicates high potassium, thorium and uranium.

From the ternary map, it can be seen that the sedimentary region which is at extreme south-eastern section of the map is black in colour which indicates low potassium, thorium and uranium. A thin light blue strip (cyan) observed in the sedimentary region suggests small intrusion of uranium rich minerals in the sedimentary rock. The biotite granite rock located at Latitude 8.44^{o}N-8.50^{o}N and Longitude 8.20^{o}E-8.30^{o}E and the same rock located at Longitude 7.46^{o}-8.04^{o}E and Latitude 8.30^{o}-8.34^{o}N show relatively high content of K, Th and U .The medium to coarse grained biotite-granite which shows red on the ternary map indicates a potassium rich rock. This region is a region of hydrothermal alteration. This is because according to the geology map of the area, the rock type just above this area is also a biotite-granite which has a high amount of the three radioactive elements. Therefore, there is a possibility that Potassium enrichment took place, thereby depleting the Uranium and Thorium content of that rock. This area corresponds to what was seen in the Potassium/Thorium ratio map (Figure 4.13).

Another striking feature in the ternary map is the lineament located towards the south-western region of the map at Longitude7.24^{o}- 7.25^{o}E and Latitude 8.30^{o}-8.50^{o}N.This lineament which appears reddish in the map can be interpreted as region of hydrothermal alteration. This is because the lineament has been enriched with potassium at the expense of thorium and uranium. This is also because the area where the lineament is located are rocks rich in thorium and uranium as seen in the ternary map. Therefore hot aqueous potassium laden fluids passed through the lineament and depleted thorium and uranium.

Furthermore, the intrusive bodies labelled A1 and A2 in the FVD along with some pockets of intrusions show an enrichment of potassium. On the other hand, the intrusive biotite-granite rock labelled A3 and A4 in the FVD map has high content of all the three radioactive elements. This region appeared whitish in the ternary map. Another feature that cannot be overlooked is a curved stripe reddish brown colour band observed around the south-western axis at Longitude 7.14^{o}E-7.16^{o}E and Latitude 8.30^{o}N-8.47^{o}N.This curved stripe was also seen in the K/Th and K/U ratio maps and it delineates change in lithology.

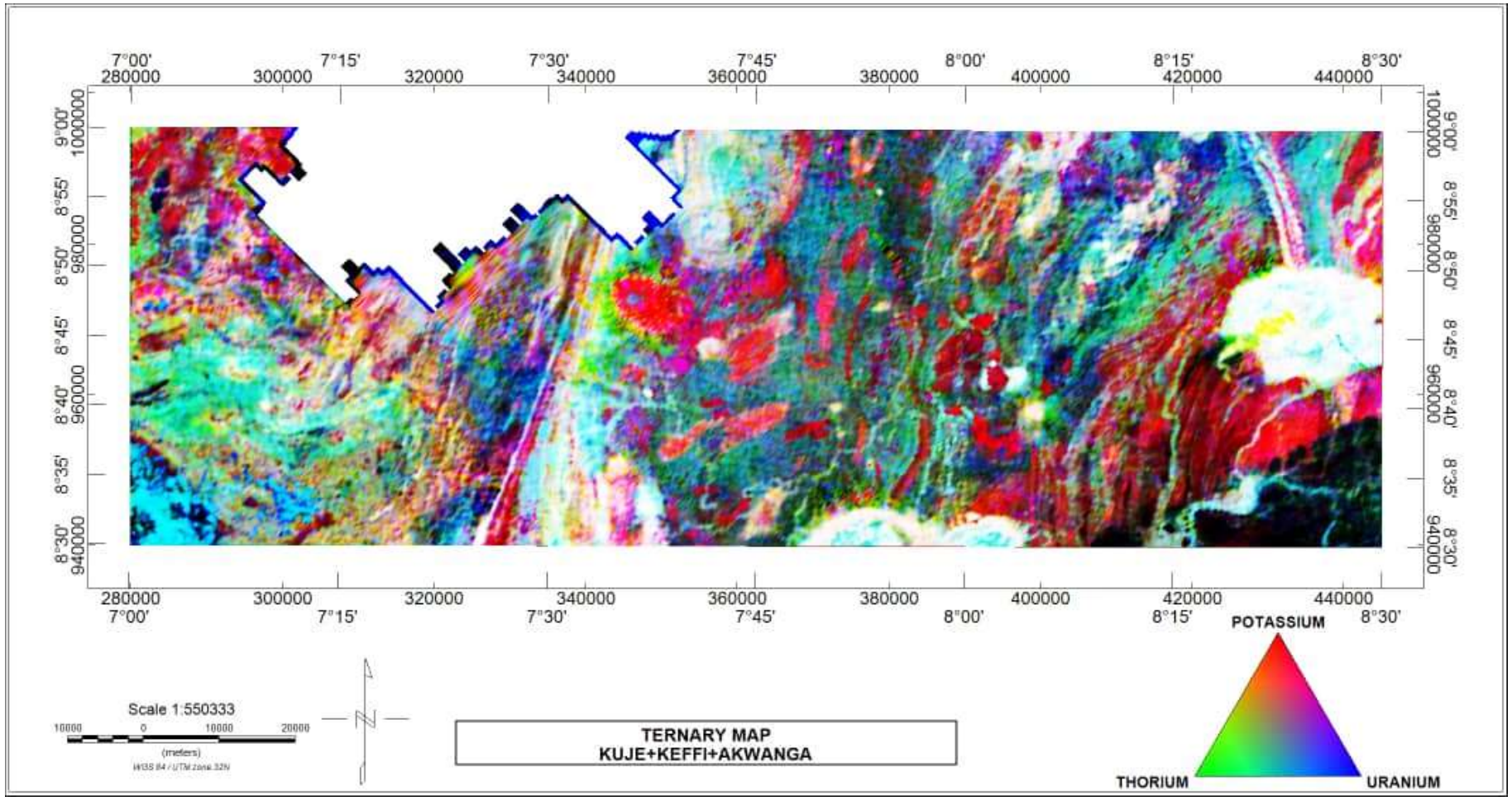

Figure 4.18: Ternary Map of the Study Area.

CHAPTER FIVE

5.0 CONCLUSION AND RECOMMENDATIONS

5.1 Conclusion

The analysis of the aeromagnetic data using various filtering techniques was very useful in mapping faults, folds, lineaments, contacts and intrusions which are likely regions of mineral accumulation. The residual magnetic intensity map shows that the high magnetic signature occupies mostly the north-eastern and the south-western region of the map while the extreme south-eastern and north-western region have low magnetic signatures.

The short wavelength of magnetic signatures seen in the western end, some parts of the central and south-eastern part of the horizontal derivative maps are characteristics of outcrops and shallow intrusions that are weathered. On the other hand, the long wavelength observed at the extreme south-eastern end of the horizontal derivative map is an indication of area with thick sedimentation.

A critical look at the First vertical derivative map shows pockets of intrusions but the major intrusive bodies were labelled A1, A2, A3 and A4 which coincides with the porphyritic granite, undifferentiated granite and muscovite schist, biotite granite and medium to coarse grained biotite granite rock respectively in the geology map. Faults were mapped out on the south-western and the south-eastern part of the map. Also series of lineaments were observed but the major ones were mapped on the south-western (Longitude 7.24^0E-7.25^0E and Latitude 8.30^0N-8.50^0N) and the north-eastern part of the map. Furthermore, the first vertical derivative map revealed the occurrence of fold in the boundary between the basement and the sedimentary rock at the south-eastern end as well as the intrusive bodies marked A3 and A4.

The analytical signal map reveals bodies with high susceptibility appearing as isolated spherical or round shapes which coincides with granitic bodies.

The K/eTh ratio map revealed the region of hydrothermal alteration to be the region that coincides with the medium to coarse grained biotite granite rock which share a common boundary with the sedimentary rocks at the extreme south-eastern end of the map. This region is delineated as region of hydrothermal alteration because the same rock type located above it which is biotite granite and located at Latitude 8.44^{o}N-8.50^{o}N and Longitude 8.20^{o}E-8.30^{o}E while the medium to coarse –grained biotite granite which is altered has high K/eTh ratio. This is because Th has been mobilized and depleted with the resultant enrichment of K.

The ternary map revealed that the biotite granite rock located at Latitude 8.44^{o}N-8.50^{o}N and Longitude 8.20^{o}E-8.30^{o}E and that located at Longitude 7.46^{o} E – 8.04^{o}E and Latitude 8.30-8.34^{o}N have relatively high K, U and Th content.

The region of hydrothermal alteration as indicated in the K/Th map is confirmed in the ternary map. The biotite granite rock located at Latitude 8.40^{o}N-8.43^{0}N and Longitude 8.20^{o}E-8.30^{o}E shows potassium enrichment while the same rock type above it shows relatively high concentration of K, Th and U. Therefore hot aqueous mineral laden fluids rich in potassium must have altered the mineralogy of the host rock. This region of hydrothermal alteration was correlated with the First vertical derivative map and faults were found in this region. These faulted rocks served as channels for hydrothermal fluid to flow.

Another region of hydrothermal alteration found in the ternary map is the lineament located towards the south-western area of the map located towards the south–western area of the map at Longitude 7.24^{o}E-7.25^{0}E and Latitude 8.30^{o}N-8.50^{o}N .The map shows potassium enrichment of the lineament at the expense of the surrounding rocks

which shows varying concentration of the three elements. Furthermore fractures show up as magnetic lineaments on FVD maps. The magnetic lineaments that represents fractures where hydrothermal alteration took place are potential hosts of gold minerals. Such fractures are located in the area of high residual magnetic anomaly. Rocks in areas of high magnetic anomaly, associated with these fractures are probably conduits for mineral accumulation. The probability of hosting gold is enhanced when they are associated with high K/Th ratio, which is observed in the K/Th ratio map. These regions of hydrothermal alteration are the areas of promising mineralization.

5.2 Recommendations

Ground-truthing should be carried out by the appropriate geological setting especially in the area delineated as gold mineralized zones which are located at Latitude 8.40^{o}N-8.43^{0}N, Longitude 8.20^{o}E-8.30^{o}E and Longitude 7.24^{o}E-7.25^{0}E, Latitude 8.30^{o}N-8.50^{o}N in order to ascertain the quality and relative abundance of the various solid minerals found in the area.

REFERENCES

Ademila, O., Akingboye, A. S., and Ojamomi A. I. (2018). Radiometric survey in geological mapping of parts of basement complex area of Nigeria. Vietnam journal of Earth Sciences, 40(3), 288-298.

Adetona, A.A. and Abu, M. (2013). Investigating the structures within the lower Benue and Upper Anambra Basins Using First Vertical Derivative, Analytical Signal and Centre for Exploration Targeting (CET) plug-in. Earth science. Volume 2, No.5, 2013, 104-112.doi:10.11648/j.earth.20130205.11.

Adewumi, T., & Salako, K.A. (2017). Delineation of mineral potential zone using high resolution aeromagnetic data over part of Nasarawa state, North Central Nigeria. *Egyptian journal of petroleum* 27 (2018) 759-768.

Ahmed, S.A., Ahmed, A.E, Ashraf, E.G., Sami, H.A., Marwan, A.A., (2012). Application of aeromagnetic data to detect the basement tectonics of eastern Yemen region. *Egyptian Journal of Petroleum,* 22, 2777-292

Aina, A. and Olarewaju, V. O, (2010). Geological Interpretation of Aeromagnetic Data in some Parts of North-central Nigeria. *Journal of Africa Earth Sciences volume iii, pp 10.*

Ajibade, A.C. & Fitches, W.R. (1988). The Nigerian Precambrian and the Pan-African orogeny. Precambrian Geology of Nigeria. Geological Survey of Nigeria, pp. 45-53.

Akanbi, E.S and Udensi, E. E., (2006). Structural Trends and Spectral Depth Analysis of the Residual Field of Pategi Area, Nigeria, Using Aeromagnetic Data. *Nigeria Journal of Physics 18(2), (2006).*

Amadi, A.N., Okoye, N.O., Olasehinde, P.I., Okunola, I.A., Alkali, Y.B., Ako, T.A. and Chukwu, J.N., (2012). Radiometric Survey as a Useful Tool in Geological Mapping of Nigeria. *Journal of Geography and Geology.*Vol.4, No.1.

Appleton J.D., Miles J.C.H., Green B.M.R, Larmour R., (2008). Pilot study of the application of Tellus air-borne radiometric and soil geochemical data for radon mapping. *Journal of Environmental Radioactivity,* 99, 1687-1697.

Beard, L.P. and Goitom, B., (2000). Some problems in interpreting low latitude magnetic surveys. *Conference: 6th EAGE/EEGS meeting.*

Bierwirth P.N., (1997). The use of airborne gamma-emission data for detecting soil proper-ties. *Proceedings of the Third International Airborne Remote Sensing Conference and Exhibition. Copenhagen, Denmark.*

Clark, D. A. and Emerson, D. W. (1991). Notes on rock magnetic characteristics in applied Geophysical studies. *Exploration Geophysics, pp. 22:547–555.*

Collins, C.C., (2011). Structural Analysis of the Zaria Batholiths in the Basement Complex Northern Nigeria Using High Resolution Shallow Seismic Reflection Survey. Project: Ph.d Thesis.

Cooley, J.W. and Tukey, J.W. (1965). An Algorithm for the Machine Calculation of Complex Fourier Series.

Cooray, I. G. (1974). The Charnockitic rocks of Nigeria. Pitchamutu vol. Bangladese University, India, pp.5073.

Dalan, A.R., (2006). A Geophysical Approach to Buried Site Detection Using Down-hole Susceptibility and Soil Magnetic Techniques. *Archaeological Prospection, volume 13, issue 3, pages 182-206.* http://doi.org/10.1002/arp.278/.

Daniel, E., Jimoh,R. and Lawal, K.,(2019). Delineation of Gold Mineral Potential Zone Using High Resolution Aeromagnetic Data over Part of Kano State, Nigeria. *Journal of Geology and Geophysics 8:464.10.35248/2381-8719.464.*

Darnley, A. G., and Ford, K. L., (1989). Regional airborne gamma-ray survey: A review; in "Proceedings of Exploration 87: Third Decennial International Conference on Geophysical and Geochemical Exploration for Minerals and Ground Water", Geological Survey of Canada, Special, pp. 960.

Darnley, A.G. (1972). Airborne Gamma-ray Survey Techniques. In: Bowie *et al.*, (Editors), Uranium Prospecting Handbook. Institute of Mining and Metallurgy, London, pp 174-211.

Darnley, A.G. (1973). Airborne Gamma-ray Survey Techniques- Present and Future; Uranium Exploration Methods. International Atomic Energy Agency, Proceedings of a Panel, Vienna, 67-108.

Dearing J.A, (1994). Environmental magnetic susceptibility, using the Bartington MS2 system.

Debeglia, N., and Corpel, J. (1997). Automatic 3-D interpretation of potential field data using analytic signal derivatives, Geophysics 62 (1) 87–96.

Dickson, B.L. and Scott, K.M. (1997). Interpretation of aerial gamma ray surveys; adding the geochemical factors. *Journal of Australian geology and geophysics*

Dobrin, M.B. and Savit, C.H. (1988). Introduction to Geophysical Prospecting. 4th Edition, McGraw-Hill, New York, 867p.

Durrance, E.M., (1986). Radioactivity in geology, principles and applications: Ellis Horwood Ltd., 441p.

Ejepu, J. S., Unuevho, C. I., Ako, T. A and Abdullahi,S.(2018). Integrated Geosciences Prospecting for Gold Mineralization in Kwakuti, North-Central Nigeria. *Journal of Geology and mining Research.* Vol. 10 (7), pp 81-94. Article Number: 774953558587. ISSN: 2006-9766.

Ekeleme, I.A., Uzoegbu, M.U., Olorunyomi, A.E, Abalaka, I.E, (2017).The Geologic Investigations of Rocks around Angwan Madaki and its evirons, North Central Nigeria. *International Journal Geology and Mining* 3(1): 090-102.

Ekwueme BN (2003). The Precambrian Geology and Evolution of the South eastern Nigerian Basement Complex, University of Calabar Press 240pp.

Elawadi, E., Ammar, A., and Elsirafy, A., (2004). Mapping surface geology using airborne gamma ray spectrometric survey data - A case study. *Proceedings of SEGJ international symposium. Nuclear Materials Authority of Egypt, Airborne Exploration Dept.*

Falconer, J. D. (1911). The geology and geography of Northern Nigeria. Macmillan, London, 135pp.

Faure, G. (1977). Principles of Isotope Geology. UK: John Willy and Sons Inc. 331p.

Galbraith, J. H. and Saunders, D. F. (1983). Rock classification by characteristics of aerial gamma-ray measurements. *Journal of geochemical exploration*, Vol.**18**, No. 1., pp.49-73.

Grant, N.K., (1978). Structural Distinction between a Metasedimentary Cover and an Underlying Basement in the 600 m.y-old Pan-African Domain of North-western Nigeria, West Africa. Bull Geol Soc America 89:50-58.

Hoover, D.B., Heran, W.D. and Hill, P.L. (1992). The Geophysical Expression of Selected Mineral Deposit Models. U.S. Geological Survey Open-File report 92–557, pp. 129.

Idzi, A., Olaleke A. and Etonihu, A.C (2013). Geochemical Studies of Mineral Bearing Ores from Nasarawa Eggon and Udege Beki Areas of Nasarawa State, Nigeria. International Journal of Basic and Applied Sciences volume 3(issue 1): pp 93-108.

International Atomic Energy Agency (IAEA), (1991). Airborne gamma ray spectrometer surveying, International Atomic Energy Agency, Technical Report Series, 323.

International Atomic Energy Agency (IAEA), (2003). Guidelines for radioelement mapping using gamma ray spectrometry data, Vienna.

Jacobson, R., and Webb, J.S., (1964). The Pegmatite of Central Nigeria, Geological Survey of Nigeria; Bulletin (17): pp.1-60.

Jones, H.A and Hockey, R.D (1964). The Geology of Part of South-western Nigeria. Geological Survey of Nigeria Bulletin. Pp 31, 1-101.

Joseph, O.O., Oniku, A.S., Meludu, O.C, Mathew, O.M., and Usman,A.,(2019). Interpretation of Aeromagnetic and Satellite Data over Part of Maru Schist Belt, North-western Nigeria. *Journal of Geology and Geophysics 7:457.doi:10.4.72/2381-8719.1000457.*

Kearey, P., Brooks, M., Hill, I., (2002). An introduction to geophysical exploration third Edition. TJ international. pp. 2-16

McCurry, P., (1976). The geology of the Precambrian to lower Palaeozoic Rocks of Northern Nigeria –A review In: Kogbe C.A (ed) Geology of Nigeria. Elizabethan Publishers, Lagos pp15-39.

Milligan, P.R. & Gunn, P. J., (1997). Enhancement and presentation of airborne geophysical data, AGSO *J. Geol. Geophys*. 17 (2) (1997) 63–75.

Milsom, J., (2003). Field Geophysics, the Geological Field Guide Series. Third edition. John Wiley and sons Limited, The Atrium, Southern Gate, Chichester, pp.71.

Minty, S., (1996). Calibration and Data Processing for Airborne Gamma-ray Spectrometric Data. *Journals of Australian Geological Survey Organisation., vol 19, issue 6.*

Nabighian, M. N., (1972) .The analytic signal of two-dimensional magnetic bodies with polygonal cross-section: Its properties and use for automated anomaly interpretation, *Geophysics 37 (3) 507–517.*

Nabighian, M.N., (1984). Toward a three-dimensional automatic interpretation of potential field data via generalized Hilbert transforms: fundamental relations. *Geophysics 49(6), 780–786.*

Nettleton, L.L.,(1962). Elementary gravity and magnetics for Geologists and Seismologists: Society of Exploration Geophysicists Monograph series 1, pp .121.

Nwankwoala, H. O., Ugwo, S. A., & Agada E.A., (2017). Interpretation of Aeromagnetic Survey and Satelite Imagery of Jos –Plateau, North-Central Nigeria. *International Journal of Emerging Engineering Research and Technology, volume 5, ISSUE 3, March 2017, Pp 1-9. ISSN 2349-4395.*

Obaje, N. G., Jauro, A., Agho, M.O., Abubakar, M.B., Tukur, A.,(2007). Organic Geochemistryof Cretaceous Lamza and Chikila coals, Upper Benue Trough, Nigeria. *Fuel 86(4) 520-532*

Obaje, N. G., (2009). Geology and mineral resources of Nigeria. Springer Dordrecht Heidelberg London New York, 221pp.

Obi, D. A., Ilozobhie, A. J., & Abua, J.U., (2015). Interpretation of aeromagnetic data over the Bida Basin, North Central Nigeria. Pelagia Research Library. Advances in Applied Science Research 6(3):50-63.

Obiora, S.C., (2005). Field Description of Hard Rocks with examples from the Nigerian Basement Complex 1st (ed.) swap Press (Nig.) Ltd Enugu, 14pp.

Ogunmola, J. K., Gajure, E. N., Ayolabi, E. A, Olabaniyi, S. B., Jeb, D. N and Agene, I. J, (2015). Structural study of Wamba and Environs North-central Nigeria using Aeromagnetic data and Nigeria Sat-X Image.

Ohioma, J.O., Ezomo, F.O., and Akinsumade, A., (2017). Delineation of Hydrothermally Altered Zones that Favour Gold Mineralization in Isanlu Area,

Nigeria using Aero-radiometric Data. *Journals of International Annals of Science ISSN: 2456-7132 volume 2, issue 1, pp. 20-27.*

Okezie, C. N., (1974). Geological Map of Nigeria. Geological Survey of Nigeria. Elsevier Ltd. Pp. 6.

Olomo, K.O., Olayanju, G.M., Adiat K.A.N. and Akinlalu, A.A, (2018).Integrated Approach Involving Aeromagnetic and Landsat for Delineating Structures and its Implication on Mineralization. *International Journal of Scientific and Technology Research volume 7 issue 2.*

Oyawoye M. O., (1964). The geology of Nigerian Basement Complex. *Journal of Nigeria Mining, Geol. And metal society,* 1: pp. 87-102.

Ozebo, V.C., Ogunkoya, C., Makinde, V. and Layade, G., (2014). Source Depth Determination from Aeromagnetic Data of Ilesha, Southwest Nigeria, Using the Peters' Half Slope Method. Earth Science Research 3(1):152-162. DOI: 10.5539/esr.v3n1p41

Portnov, A.M. (1987). Specialization of Rocks toward Potassium and Thorium in Relation to Mineralization. International Geological Review, vol. 29, pp. 326–344. https://doi.org/10.1080/00206818709466149.

Rahaman, M.A (1988). Recent Advances in the Study of the Basement Complex of Nigeria in Precambrian Geology of Nigeria, Geological Survey of Nigeria, Kaduna South. Pp 11-43.

Rajagopalan, S., (2003). Exploration Geophysics, 34(No. 4): pp. 257-262.

Reeves, C. V., (1989). Aeromagnetic interpretation and rock magnetism. First Break, 7: pp.275– 286.

Reeves, C.V., (2005). Aeromagnetic Survey Principles, Practice and Interpretation. *Geosoft*, pp1.

Reeve W. D., (2010) .Geomagnetism Tutorial. Reeve Observatory Anchorage, Alaska-USA.

Reid, A.B., Allsop, J.M., Granser, H., Millet, A.J., Somerton, I.W., (1990). Magnetic interpretation in three dimensions using Euler deconvolution. Geophysics 55, 80–91.

Reynolds J. M., (1997). An introduction to Applied and Environmental Geophysics, John Wiley & Ltd. Bans Lane, Chichester. pp. 124-132.

Rowland, A. A and Nur, A., (2018). Structural Patterns Deduced from Aeromagnetic Data over Parts of Nasarawa and Environs Northcentral Nigeria. *Global Journal of Geological Sciences* Vol.17, 2019:85-95.

Roy, K.K., (2018). Potential Theory in Applied Geophysics. Pp 30.

Salako, K.A., and Udensi, E.E, (2013). Spectral Depth Analysis of Part of Upper Benue Trough and Bornu Basin, North-east Nigeria, using Aeromagnetic Data. *International Journal of Science and Research 2 (8).*

Sayeed, O.E. and Mahmoud, A.G. (2018). Delineation of Potential Gold Mineralization Zones in a Part of Central Eastern Desert, Egypt Using Airborne Magnetic and Radiometric Data. *NRIAG Journal of Astronomy and Geopphysics.*

Slagstad, T. (2008). Radiogenic Heat Production of Archean to Permian Geological Provinces in Norway. *Norwegian Journal of Geology/Norsk Geologist Forening* 88(3).Pp 123.

Talaat, M. R and Mohammed F.A. (2010). Characterization of Gold Mineralization in Garin Hawal Area, Kebbi State North-west Nigeria using remote sensing. *The Egyptian journal of remote sensing and space sciences* (2010) 13, 153-163.

Telford, W. M., Geldart, L. P., and Sheriff, R. E. (1990). Applied Geophysics. Cambridge University Press, second edition. Pp 356.

Thompson, D.T., (1982). EULDPH – a new technique for making computer-assisted depth estimates from magnetic data. Geophysics 47, 31–37.

Umeji, A. and Caen-Vachette, M., (1991). Geochronology of a Rhyolite Dyke from Nassarawa-Eggon in Central Nigeria. Geologische Rundschau.80.10.1007/ BF01828774.

Uwah, J. E., (1984). Investigation of radiometric anomalies by nuclear and other methods. (A case study of the Sokoto basin of Nigeria). Unpublished Ph.D Thesis, Department of Physics, Ahmadu Bello University, Zaria, pp 1-135.

Wemegah, D.D., Menyeh, A., and Danuor, S.K., (2009). Magnetic Susceptibility Characterization of Mineralized and Non-mineralized Rocks of the Subenso Concession of Newmont Ghana Gold Limited. Ghana Science Association Biennial Conference. pp.45.